Radiative Gluon Emission via MHV Techniques

Tanjona Radonirina Rabemananjara (radonirina@aims.ac.za)
African Institute for Mathematical Sciences (AIMS)

Supervised by: Dr. W. A. Horowitz
University of Cape Town, South Africa

18 May 2017

Submitted in partial fulfillment of a structured masters degree at AIMS South Africa

Abstract

We introduce the study of the energy loss of an energetic light quark passing through an interacting Quark-Gluon Plasma. Using recent mathematical tools to compute tree-level scattering amplitudes in massless gauge theories, we calculate the cross section and the momentum distribution of the radiative gluons emanating from the $qg \to qg$ process. We see that for the case of one radiative gluon emission, the distribution converges to the Poisson distribution. For two gluon emission, a correction term has to be added to the Poisson distribution. In building towards the study of radiative Bremsstrahlung gluons, we derive the general formula for the Maximally Helicity Violating (MHV)-amplitude of a QCD process with exactly one pair of quark anti-quark and a certain number of gluons.

Declaration

I, the undersigned, hereby declare that the work contained in this research project is my original work, and that any work done by others or by myself previously has been acknowledged and referenced accordingly.

Tanjona Radonirina Rabemananjara, 18 May 2017

Contents

1. Introduction

It has long been recognized that a microsecond after the big bang the universe was filled with a new state of matter in which quarks and gluons are deconfined (Heinz and Jacob, 2000). Quarks and gluons, moving at near the speed of light, formed an ultra-hot and dense soup called the Quark Gluon Plasma (QGP). Experimental attempts to reproduce similar conditions have been conducted at experiment accelerators by making head-on collisions between heavy-ions (Armesto and Scomparin, 2013). The first evidence of a QGP was seen in 2003 at Brookhaven National Laboratory's Relativistic Heavy Ion Collider (RHIC). With a center of mass energy of $\sqrt{s_{NN}} = 200\,GeV$, scientists at RHIC reached the hottest temperature ever produced in a laboratory, about $250\,000$ times the temperature of the center of the sun (Adler et al., 2003). Scientists expected the QGP to behave like a gas of free quarks, anti-quarks and gluons (Back et al., 2005). Surprisingly, as opposed to what scientists expected the soup made of quarks and gluons has a verly large elliptic flow v_2, so it therefore behaves as a near perfect fluid $(\eta/s \sim 1/4\pi)$ (Jacak and Steinberg, 2010). Furthermore, recent experiments at the European Organization for Nuclear Research (CERN) and RHIC have shown a depletion of high transverse momentum $(p_\perp)$ hadrons , known as *jet quenching* (Aad et al., 2010; Adams et al., 2005).

The term jet quenching refers to the modification of an energetic parton due to its interactions with the medium (Armesto et al., 2012). Data collected at heavy-ion experiments at RHIC and LHC suggest that jet quenching is a consequence of the energy loss of the primary parton (Wang, 2004). In spite of significant development in explaining the energy loss phenomena, the mechanism is not fully understood. The energy loss is expected to occur via elastic (*collisional energy loss*) and/or inelastic (*radiative energy loss*) processes (Andronic et al., 2016). The idea of *collisional energy loss* of high momentum particles in high energy collisions was pioneered by Bjorken (1982), in which an energetic parton loses energy through elastic collisions with the particles composing the medium. Another energy loss channel can be from the energetic parton radiating gluons (gluon Bremsstrahlung) induced by collisions with medium particles as studied by Wang (2005) and Chen et al. (2010). In heavy-ion collisions, the interaction between a high energy parton and a thermal gluon can yield the emission of gluon radiations and the decrease of the energy of the parton (Baier et al., 2000). Since interacting with medium particles, the study of the parton energy loss provides insight into the dynamics of the QGP.

Theoretically, at high-momentum the physics of a QGP is thought to be governed by the weak-coupling physics of Quantum Chromodynamics (QCD) (Collins and Perry, 1975; Vitev, 2006). Indeed, due to the asymptotic freedom of QCD quark and gluon interactions become very weak at high energy (Gross and Wilczek, 1973; Politzer, 1973). As investigated in Wicks et al. (2007) and Fochler et al. (2009), study of jet quenching can be therefore approached using perturbative QCD (pQCD).

The aim of the project is to evaluate the distribution of radiative gluons emitted from an energetic light quark. This momentum distribution is an important step toward the understanding of the parton energy loss. Theoretically, physical processes, represented by its scattering amplitude, are often approached with conventional Quantum Field Theory using Feynman diagrams. However, it turns out that the calculation using Feynman diagrams gets extremely complicated as the number of external particles increases. Indeed, calculations with Feynman diagrams are realizations of a perturbative expansion: when doing calculations with Feynman diagrams, one has to set up all topologically different diagrams for a given process up to a given order of coupling in the theory (Henn and Plefka, 2014). This process very quickly makes calculations of scattering amplitudes complicated. As an illustration, Table 1.1 shows the factorial growth of the number of Feynman diagrams needed for the tree-level scattering amplitude of n gluons.

n	4	5	6	7	8	9	10
♯ Diagrams	4	25	220	2.485	34.300	559.405	10.525.900

Table 1.1: Number of Feynman diagrams involved in a process as a function of the number of external particles (Parke and Mangano, 1991).

Recently, a number of new approaches have been developed for the computation of multi-parton matrix elements in gauge theories. One of the methods includes the *spinor helicity formalism*. This formalism was introduced because the Lorentz group $SO(1,3)$ in four dimensions is isomorphic to $SL(2) \times SL(2)$, and hence the finite-dimensional representations are classified as (m,n), where m and n are integers or half-integers (Witten, 2004). The color-kinematic decomposition comes from the fact that a QCD-amplitude can be factorized into a color term and a gauge invariant color-ordered amplitude (Dixon, 2014; Henn and Plefka, 2014). In addition, while studying the properties of scattering amplitudes, *on-shell recursion relation* has been discovered (Feng and Luo, 2012). The idea is that all the amplitudes can be constructed from the most basic and simplest amplitude (3-point amplitude).

In this essay, we propose to study the QCD process $qg \to qg + ng$ where $n = 0, 1, 2$ is the number of bremsstrahlung gluons. In Chapter 2 we introduce the basic idea of color decomposition and the spinor helicity formalism. Then, we introduce a specific on-shell recursion called the Britto-Cachazo-Feng-Witten (BCFW) relation. Chapter 3 focuses on the computation of the scattering amplitude of the parent process $qg \to qg$. We also prove the general partial amplitude formula for processes involving external quarks. In Chapter 4, we use the process $qg \to qg$ as a building block to compute the case where we have a Bremsstrahlung gluon and to evaluate the probability that this radiated gluon is emitted. In Chapter 5 we propose a generalization for a higher number of radiative bremsstrahlung gluons and give a conclusion.

2. Background theory

Scattering amplitudes are an important observable in quantum field theory. They are essential for making theoretical predictions about particle physics experiments. Theoretically, scattering amplitude describes the probability for a process to occur. The result is then compared to the measured probabilities if it is consistent. The most conventional way of doing the calculation of these scattering amplitudes is the use of Feynman diagrams. However, this method turns out to be very complicated while computing large number of particles. The reason is because Feynman diagrams involve *off-shell* (or virtual) *particles*. This section consists of introducing new techniques for computing *on-shell scattering amplitudes*.

2.1 Color-kinematic decomposition

Although the gauge group of quantum chromodynamics is $SU(3)$, let us generalize it to $SU(N)$ where the color indices run over $1, 2, \cdots, (N^2-1)$. The generators T^a are normalized such that $Tr(T^aT^b) = \delta^{ab}$ and $[T^a, T^b] = i\sum_{c=1}^{N^2-1} \tilde{f}^{abc}T^c$. For our normalization, $\tilde{f}^{abc} = \sqrt{2}f^{abc}$ where f^{abc} is the structure constant. Using Einstein's notation, we can just write $[T^a, T^b] = i\tilde{f}^{abc}T^c$. To expose the color structure of the scattering amplitudes, we first eliminate the structure constant $\tilde{f}^{abc}$ in favor of the generator T^a. According to the last relation we have

$$i\tilde{f}^{abc} = Tr(T^aT^bT^c) - Tr(T^aT^cT^b). \tag{2.1.1}$$

Thus, for a pure gluon process the color term in the amplitude involves a product of traces. If we have a presence of external quarks, then in addition to the traces there will be a term of the form $(T^{a_1}\cdots T^{a_n})_{ij}$, where i and j are the fundamental indices such that $i, j = 1, \cdots, N$. On the other hand, the matrices of the fundamental representation of $SU(N)$ satisfy the following identity:

$$(T^a)_{ij}(T^a)_{kl} = \delta_{il}\delta_{kj} - \frac{1}{N}\delta_{ij}\delta_{kl}. \tag{2.1.2}$$

This is known as the *Fierz identity* and the term proportional to N^{-1} reflects the fact that the generator matrices T^a are traceless. Using this decomposition it turns out that for any process involving fermions and gluons, we can separate the color from the kinematic part. The color-kinematic decomposition of n gluons tree amplitude with two external fermions (quark anti-quark pair) Dixon (2014) is given by

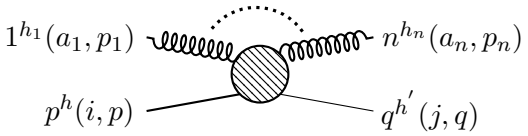

Figure 2.1: Diagrammatic representation of the $q\bar{q}g\cdots g$ process.

$$\mathcal{A}_{n+2}(p, 1, \cdots, n, q) = g_s^n \sum_{\sigma\in S_n} (T^{a_{\sigma(1)}}\cdots T^{a_{\sigma(n)}})_{ij}\, A_{n+2}[p^h, \sigma(1^{h_1}), \cdots, \sigma(n^{h_n}), q^{h'}], \tag{2.1.3}$$

where p and q denote the quark and the anti-quark respectively, and the numbers refer to the gluons. The sum is over all possible permutations of n gluons. Note that in this color basis the indices of the quark and the anti-quark are fixed and do not participate in the permutation. We say that the color indices start from the quark, pass through the gluons and end up with the anti-quark. Here $A[p^h, 1^{h_1}, \cdots, n^{h_n}, q^{h'}]$

♯ Particles	4	5	6	7	8	9	10
♯ Diagrams Partial amplitude	3	10	36	133	501	1991	7335
♯ Diagrams Full amplitude	4	25	220	2485	343000	559405	10525900

Table 2.1: Number of diagrams that contribute to the partial and full amplitude (Maltoni et al., 2014). The first row indicates the number of particles involved in the process. The second and the third row make the comparison between the number of diagrams contributing respectively for the partial and full amplitude.

are called *partial* or *color-ordered amplitudes* which only depends on the kinematics. The color factor tells the order in which the gluon are emitted. A comment on the notation in (2.1.3) is that particles are labeled by i (except for the quarks) which carry color indices a_i and momentum p_i. We write the helicity label for each particle, $h_i = \pm$, as a superscript. The computation of tree amplitudes in Yang-Mills theory has now been reduced to the computation of partial amplitudes. Table 2.1 gives a brief overview of how efficient is the computation of partial amplitude compared to the full amplitude.

The color-kinematic decomposition provides a good organization of the colors in the expression of scattering amplitudes, where we are now left with the computation of partial amplitudes. However, these gauge invariant partial amplitudes are easier to compute compared to the direct computation of the full amplitude, since they are color ordered. In addition, their expression can be derived in a much more efficient way using new mathematical tools, such as the spinor helicity formalism and the BCFW on-shell recursion (see Section 2.3), especially for a large number of external particles.

Moreover, partial amplitudes present interesting properties:

- Charge conjugation $A[p, 1, \cdots, n, q] = -A[q, 1, \cdots, n, p]$. Flipping charges on a quak anti-quark line gives rise to a minus sign.
- Cyclic in the sense that $A[1, 2, \cdots, n-1, n] = A[n, 1, 2, \cdots, n-1]$. This is an immediate consequence of color-ordered amplitudes.
- Color-ordered identity, $A[1, 2, \cdots, n-1, n] = (-1)^n A[n, n-1, \cdots, 2, 1]$, this follows from the antisymmetry of color-ordered amplitudes.
- Parity under change $h_I \to h_{-I}$, $A[1, 2, \cdots, n-1, n] = A^*[1, 2, \cdots, n-1, n]_{h_I \to h_{-I}}$. This is because flipping the helicity of particles changes the angle brackets into square brackets and vice-versa. We will have a particular look at this property in the Section 4.2.

2.2 Spinor helicity formalism

2.2.1 Spinor notation. It has been noticed that in quantum field theory there is much redundancy among momenta and polarizations in the calculation of scattering amplitudes using Lorentz 4-vectors, especially when one has to deal with particles with spin. It appears that using the helicity basis one can organize efficiently the spin quantum numbers of the external states. In addition, in high energy processes particles behave as if they are massless. Massless particles interacting through gauge interactions a have conserved helicity which we can exploit by computing in the helicity basis. Although vector particles like photons and gluons do not have conserved helicity, it turns out that most helicity-violating processes one can imagine are zero at tree level.

As a basic kinematic variable for scattering amplitudes, we often use the momentum four-vector p^μ and their Lorentz invariant products $s_{ij} = (p_i + p_j)^2$. However, we can write the momentum as *bispinors*, $p_{a\dot{a}} = p_\mu(\sigma^\mu)_{a\dot{a}}$, where $\sigma^\mu = (\sigma^0, \sigma^j)_{j=1,2,3}$ are the usual Pauli matrices. Choosing a $(+---)$-signature, consider a momentum four-vector p^μ defined as $(p^0, p^j)_{j=1,2,3}$ and satisfy $p^\mu p_\mu = m^2$, then

$$p_{a\dot{a}} = p^0\sigma^0 - p^j\sigma^j = \begin{pmatrix} p^0 - p^3 & -p^1 + ip^2 \\ -p^1 - ip^2 & p^0 + p^3 \end{pmatrix}. \tag{2.2.1}$$

The determinant of this matrix which is Lorentz invariant is given by $\det p_{a\dot{a}} = p^\mu p_\mu = m^2$. In a special case where the momentum is lightlike, we find that $\det p = 0$. Indeed, since we want to compute scattering amplitudes for massless particles, it is convenient to set $m = 0$.

From linear algebra, any 2×2 matrix with zero determinant can be written as an outer product of two vectors. Thus, for a lightlike momentum p we write

$$p_{a\dot{a}} = \lambda_a\tilde{\lambda}_{\dot{a}}, \quad (a, \dot{a} = 1, 2) \tag{2.2.2}$$

where λ_a and $\tilde{\lambda}_{\dot{a}}$ are respectively the left and right-handed spinors. For real valued momentum vectors, λ_a and $\tilde{\lambda}_{\dot{a}}$ are complex valued, but they are complex conjugates of each other, $\lambda_a^* = \tilde{\lambda}_{\dot{a}}$. It follows that given two momentum p_i and p_j, their scalar product (Zee, 2010) is given by

$$p_i \cdot p_j = \frac{1}{2}\varepsilon^{ab}\varepsilon^{\dot{a}\dot{b}}(p_i)_{a\dot{a}}(p_j)_{b\dot{b}}. \tag{2.2.3}$$

The tensors $\varepsilon^{\dot{a}\dot{b}}$ and ε^{ab} can be thought of as raising and lowering spinor indices, as $g^{\mu\nu}$ does for vector indices, and their inverse are given by $\varepsilon_{\dot{a}\dot{b}}$ and ε_{ab}. Using the definition in (2.2.2) we have $(p_i)_{a\dot{a}} = \lambda_a\tilde{\lambda}_{\dot{a}}$ and $(p_j)_{a\dot{a}} = \mu_a\tilde{\mu}_{\dot{a}}$, so the product of two vectors (2.2.3) can be written as

$$2p_i \cdot p_j = (\varepsilon^{ab}\lambda_a\mu_b)(\varepsilon^{\dot{a}\dot{b}}\tilde{\lambda}_{\dot{a}}\tilde{\mu}_{\dot{b}}) = \langle p_i|p_j\rangle[p_i|p_j], \tag{2.2.4}$$

where we have defined the Lorentz invariant product using spinor helicity notation

$$\langle p_i|p_j\rangle = \varepsilon^{ab}\lambda_a\mu_b \quad \text{and} \quad [p_i|p_j] = \varepsilon^{\dot{a}\dot{b}}\tilde{\lambda}_{\dot{a}}\tilde{\mu}_{\dot{b}}. \tag{2.2.5}$$

It can be clearly seen from these relations that $\langle p_i|p_i\rangle = [p_i|p_i] = 0$ and all other brackets vanish, as an example $\langle p_i|p_j] = 0$. Note that these spinor products are antisymmetric, which means that $\langle p_i|p_j\rangle = -\langle p_j|p_i\rangle$ and similarly $[p_i|p_j] = -[p_j|p_i]$. Another useful relation is that taking the complex conjugate of the Lorentz invariant $\langle p_i|p_j\rangle$ gives $[p_i|p_j]$ and vice versa. The Lorentz invariant product in terms of momentum four-vector $s_{ij} = (p_i + p_j)^2$ can now be written in terms of spinor notation as

$$s_{ij} = \langle ij\rangle[ij], \tag{2.2.6}$$

where here, for simplification, we used the short-hand notation $\langle p_i|p_j\rangle = \langle ij\rangle$ and similarly $[p_i|p_j] = [ij]$. In particular, for two-to-two processes $1 + 2 \to 3 + 4$, the s_{ij} define the *Mandelstam variables* s, t, u where $s = s_{12}$, $t = s_{13}$ and $u = s_{14}$ if we consider all the momenta to be **outgoing**. Using short-hand notation, angle and square brackets are related to each other with the relation $\langle ij\rangle^* = [ij]$.

2.2.2 Correspondence in relation. Now, we need to make a correspondence between the 2-component Weyl spinors λ_a and $\lambda_{\dot{a}}$, and the 4-component Dirac spinors. Indeed, 4-component Dirac spinors appear more often in the literature than the left and right handed Weyl spinors (see table 2.2). Recall that in the massless case, the Dirac spinors verify $u_\pm = v_\mp$ and $\bar{u}_\pm = \bar{v}_\mp$. The subscripts indicate the helicity.

According to this correspondence, a lightlike momentum p_i can be written in terms of square and angle brackets as $p_i = |i\rangle[i|$. At this point it is worth mentioning that for massless particles we do not make a distinction between fermions and anti-fermions due to the rules of crossing symmetry.

Weyl Shorthand	Weyl Spinor	Dirac Spinor
$\|i\rangle$	$\lambda_a(p_i)$	$v_-(p_i)$
$\|i]$	$\tilde{\lambda}^{\dot{a}}(p_i)$	$v_+(p_i)$
$\langle i\|$	$\lambda^a(p_i)$	$\bar{u}_-(p_i)$
$[i\|$	$\tilde{\lambda}_{\dot{a}}(p_i)$	$\bar{u}_+(p_i)$

Table 2.2: Dirac spinors and Weyl spinors correspondence. Feynman rules in terms of spinor helicity for **outgoing** massless fermions (Britto, 2015; Henn and Plefka, 2014).

2.2.3 Polarizations. The real power of the spinor helicity formalism comes when one wants to deal with vector boson polarization. Spinor helicity techniques began with the recognition that polarization vectors for massless vectors particles with definite helicity could be constructed from a pair of massless spinors.

Recall that physical polarizations satisfy the condition $\epsilon^*_\mu(p_i,k)\epsilon^\mu(p_j,k) = -1$ and the transverse condition ensures that $p_\mu\epsilon^\mu = 0$. So, our definition of polarizations expressed in terms of spinor notation has to satisfy these conditions.

As presented in Schwinn and Weinzierl (2007), the polarization vectors for massless vector bosons of definite helicity can be written as,

$$\epsilon^+_\mu(p_i,k) = \frac{1}{\sqrt{2}}\frac{\langle k|\gamma_\mu|i]}{\langle ki\rangle} \quad \text{and} \quad \epsilon^-_\mu(p_i,k) = -\frac{1}{\sqrt{2}}\frac{[k|\gamma_\mu|i\rangle}{[ki]}. \tag{2.2.7}$$

Here k is the reference momentum. The reference momentum can be chosen arbitrarily, and this freedom in choice of reference spinor reflects the gauge invariance. However, the reference momentum must not be aligned to the momentum p_i because we do not want the scalar product $k\cdot p_i$ to be zero. Since taking the complex conjugate of $\langle k|\gamma_\mu|i]$ gives $[k|\gamma_\mu|i\rangle$ and vice versa, these polarization vectors of definite helicity satisfy $(\epsilon^\pm_\mu)^* = \epsilon^\mp_\mu$. It follows straightforwardly that

$$[\epsilon^\pm_\mu(p_i,k)]^*[(\epsilon^\mu)^\pm(p_i,k)] = -\frac{1}{2}\frac{\langle k|\gamma^\mu|i]}{\langle ki\rangle}\frac{[k|\gamma_\mu|i\rangle}{[ki]}. \tag{2.2.8}$$

For the evaluation of the numerator, we need the *Fierz rearrangement* defined by Dixon (2014) as,

$$\langle i|\gamma^\mu|j]\,[l|\gamma_\mu|k\rangle = 2\langle ik\rangle[lj]. \tag{2.2.9}$$

By virtue of this relation we can compute the Equation (2.2.8),

$$[\epsilon^\mp_\mu(p_i,k)][(\epsilon^\mu)^\pm(p_i,k)] = -\frac{\langle ki\rangle[ki]}{\langle ki\rangle[ki]} = -1. \tag{2.2.10}$$

This shows that the above condition $\epsilon^*_\mu(p_i,k)\epsilon^\mu(p_j,k) = -1$ is satisfied. In addition, since $\langle ii\rangle = [ii] = 0$ it follows straightforwardly that the transverse condition $p_\mu\epsilon^\mu = 0$ is also satisfied. Similarly, we can derive the following properties for the polarizations, $\epsilon^\pm_\mu(p_i,k)\epsilon^\pm_\mu(p_j,k) = 0$ and $\epsilon^+_\mu(p_i,k)\epsilon^-_\mu(k,r) = 0$.

2.2.4 QED application. Let us now apply the formalism that we have introduced to a simple process in Quantum Electrodynamics (QED). For a concrete application consider the process $e^+e^- \to \mu^+\mu^-$ in high energy limit, represented by the tree-level diagram in Figure 2.2.

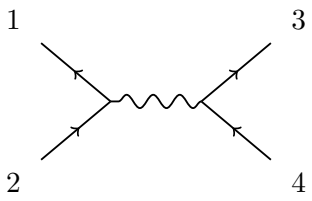

Figure 2.2: Tree-level diagram for $ee \to \mu\mu$ scattering in QED

The scattering amplitude of this diagram gives rise to a term $u_{h_2}(p_2)\gamma^\mu \bar{v}_{h_1}(p_1)$ and $\bar{u}_{h_3}(p_3)\gamma^\nu v_{h_4}(p_4)$. Choosing the electron to have a positive helicity, and since $[1\gamma^\mu 2] = 0$, the positron must have a negative helicity. Similarly, taking the muon to be $\langle 3|$, forces the anti-muon to be $|4]$. For these helicities:

$$i\mathcal{A}_4(1^-, 2^+, 3^-, 4^+) = (ie)^2 \langle 2|\gamma^\mu|1] \frac{-ig^{\mu\nu}}{\langle 12\rangle[12]} \langle 3|\gamma^\nu|4] = \frac{2ie^2}{\langle 12\rangle[12]} \langle 23\rangle[41], \tag{2.2.11}$$

where we used the *Fierz rearrangement* to obtain this expression. In order to get the cross section of this process we have to square the above amplitude,

$$|\mathcal{A}_4(1^-, 2^+, 3^-, 4^+)|^2 = \mathcal{A}_4\mathcal{A}_4^* = \frac{4e^4}{s^2} \langle 23\rangle[41][23]\langle 41\rangle = 4e^4 \frac{u^2}{s^2}. \tag{2.2.12}$$

Furthermore, we have to consider all the possible helicities. By parity of the color-ordered amplitude under change $h_i \to -h_i$, $\mathcal{A}_4(1^+, 2^-, 3^+, 4^-) = \mathcal{A}_4(1^-, 2^+, 3^-, 4^+)$. The two non-vanishing amplitudes come from $\mathcal{A}_4(1^-, 2^+, 3^+, 4^-)$ and $\mathcal{A}_4(1^+, 2^-, 3^-, 4^+)$, which are also related by parity. We can directly get the expression of $|\mathcal{A}_4(1^-, 2^+, 3^+, 4^-)|^2$ by swapping 3 and 4 in (2.2.12), thus

$$|\mathcal{A}_4(1^-, 2^+, 3^+, 4^-)|^2 = 4e^2 \frac{t^2}{s^2}. \tag{2.2.13}$$

By summing over all possibly helicities and adding the appropriate factor, we get the scattering probability, or differential cross section which, is proportional to the full amplitude square,

$$\frac{d\sigma}{dcos\theta}(ee \to \mu\mu) \;\propto\; \frac{1}{4}\sum_{hel.} |\mathcal{A}_4|^2 = 2e^4 \frac{u^2 + t^2}{s^2}. \tag{2.2.14}$$

2.3 BCFW on-shell recursion relation

Despite the fact that the spinor helicity formalism provides an efficient way to compute MHV scattering amplitudes, the computation of the k^{th} order Next-to-Maximally Helicity Violating amplitude (N^kMHV) remains complicated. Fortunately, an alternative way to avoid this complication is to compose scattering amplitudes from a product of on-shell gauge invariant subamplitudes. The most common recursion relation is called ***BCFW on-shell recursion***. The BCFW recursion, named after Ruth Britto, Freddy Cachazo, Bo Feng and Edward Witten, is a way to compute on-shell scattering amplitudes recursively. At tree level many scattering amplitudes are constructible via on-shell recursion, which elegantly encodes factorization as a physical input. The idea of the BCFW on-shell recursion is to compute higher point scattering amplitudes from lower point amplitude. The construction is based on a linear momentum shift in a complexified momentum space which allows us to evaluate the amplitude in the complex plane.

Let us consider the $n+2$-point color-ordered amplitude A_{n+2} for massless particles. The BCFW method only affects two of the momenta, say k_i and k_j, with an helicity h_i and h_j respectively, such that they

are the only one with non-vanishing shift-vectors. The shift can be defined using the spinor variables as (Feng and Luo, 2012),

$$|i] \longrightarrow |\hat{i}] = |i] + z|j], \qquad |i\rangle \longrightarrow |\hat{i}\rangle = |i\rangle, \tag{2.3.1}$$

$$|j\rangle \longrightarrow |\hat{j}\rangle = |j\rangle - z|i\rangle, \quad |j] \longrightarrow |\hat{j}] = |j]. \tag{2.3.2}$$

The hatted variables indicate the variables after shift and z is a complex number. We call such transformation an $[i, j\rangle$-shift. Indeed the shift only affects the spinor $|i]$ and $|j\rangle$. One can check that the quantity $\langle k\hat{j}\rangle$ and $[k\hat{i}]$ are linear in z while the other quantities $\langle \hat{i}\hat{j}\rangle$, $[\hat{i}\hat{j}]$, $\langle j\hat{i}\rangle$ and $[i\hat{j}]$ remain unshifted. With $\hat{k}_i = |\hat{i}\rangle[\hat{i}|$ and $\hat{k}_i = |\hat{j}\rangle[\hat{j}|$, one can check that the momentum conservation is still satisfied since $\hat{k}_i + \hat{k}_j = k_i + k_j$. For the choice of helicity, one often chooses the configuration $(h_i, h_j) = (-, +)$ for simplicity (Henn and Plefka, 2014).

Even though the BCFW recursion was initially constructed for pure gluon processes, it can be naturally extended to include fermions, but with some exceptions. In particular, one can neither shift two adjacent fermion lines of different types and the same helicity, nor two adjacent fermion lines of the same type and different helicity, nor a fermion and an adjacent gluon with the same helicity (Luo and Wen, 2005). Therefore, we can split the corresponding diagram for the on-shell scattering amplitude A_{n+2} (two of the external legs are fermions, quark and anti-quark) into two on-shell subdiagrams (see Figure 2.3), and let the shifted leg $\hat{i}$ be on the left and the shifted leg $\hat{j}$ be on the right. Indeed, we cannot split the diagrams if the shifted leg $\hat{i}$ and $\hat{j}$ belong to the same subdiagram.

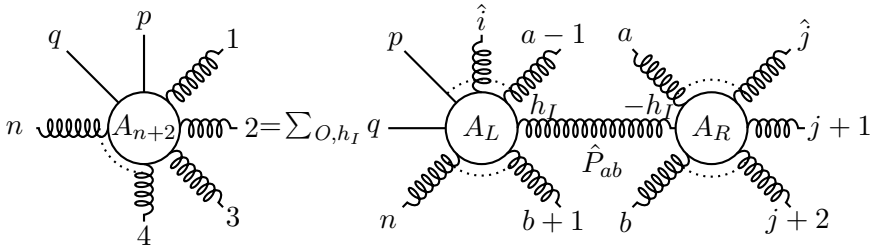

Figure 2.3: Illustration of how A_{n+2} is split into two subdiagrams via BCFW recursion.

In terms of the physical amplitude, this can be written as

$$A_{n+2} = \sum_{O} \sum_{h_I=\pm} A_L \left[1, \cdots, \hat{i}, \cdots, a-1, \widehat{P}_{ab}^{h_I}, b+1, \cdots, n\right] \frac{1}{P_{ab}^2} A_R \left[-\widehat{P}_I^{-h_I}, a, \cdots, \hat{j}, \cdots, b\right], \tag{2.3.3}$$

where $O = \{\{ab\} | i \notin \{ab\} \wedge j \in \{ab\}\}$. For a quark gluon process, the internal line can be either a gluon or a fermion line. The last case appears when p and q lie on different subdiagrams. Note that the internal momentum $\widehat{P}_{ab}$ in Figure 2.3 is on-shell ($\widehat{P}_{ab}^2 = 0$) and is given by $\widehat{P}_{ab} = k_a + \cdots + \hat{k}_j + \cdots + k_b$. The unshifted momenta P_{ab}^2 which appears in the expression of the scattering amplitude, is non-zero.

Note that each subamplitude has a number of external particles fewer than n. This recursion allows us to compute any on-shell tree amplitude in the Yang-Mills theory from lower point amplitudes. In other words we can compute 3-point amplitude, which is much easier to calculate, and apply repeatedly the BCFW recursion to construct higher point amplitudes.

3. Computation of qg to qg process

Let us now compute the cross section of the $qg \to qg$ process. In MHV-techniques we consider all the momenta to be outgoing. Thus, instead we consider the process $q\bar{q}gg$ and apply the crossing symmetry at the end. Denoted by 1 and 4 are the quark and the anti-quark, and 2 and 3 for the two gluons with color indices a_1 and a_2 respectively (see Figure 3.1). Choose p_1 to be the momentum of the incoming quark and p_4 the momentum of the anti-quark. Similarly, let us choose p_2 and p_3 to be the momentum of the two gluons. By virtue of the color-kinematic decomposition formula, the full scattering amplitude

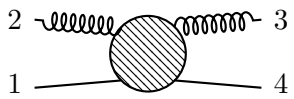

Figure 3.1: Diagrammatic representation of the $q\bar{q}gg$-process.

can be written as:

$$\mathcal{A}_4(1,2,3,4) = g_s^2 \left(T^{a_1}T^{a_2}A_4[1,2,3,4] + T^{a_2}T^{a_1}A_4[1,3,2,4]\right), \tag{3.0.1}$$

where $A_4[1,2,3,4]$ and $A_4[1,3,2,4]$ depend only on the kinematics. Let us make a choice of helicity such that we have a **Maximally Helicity Violating** (MHV)-amplitude, which means that exactly two particles must have negative helicity, say $(-,-,+,+)$. Note that the quark and the anti-quark have to have a different helicity, and due to the color decomposition, the partial amplitude for which all the gluons have the same helicity vanish. Thus, for a large number of gluons, the first non-vanishing amplitude is the case where one of the gluons has a different helicity. Since different helicities do not interfere, as shown by the color decomposition of the full amplitude, to get the full answer of the amplitude one only has to compute the squares of all the possible helicity amplitude which can contribute to the process.

3.1 Partial amplitudes

Now, let us see how the *BCFW on-shell recursion relation* is be used to compute the process. As seen in the previous section, the idea of *BCFW construction* is based on a linear momentum shift in complexified momentum space. Let us consider the $[2,3\rangle$-shift, so we get the following parametrization:

$$|\hat{2}] = |2] + z|3],\ |\hat{2}\rangle = |2\rangle \quad \text{and} \quad |\hat{3}\rangle = |3\rangle - z|2\rangle,\ |\hat{3}] = |3]. \tag{3.1.1}$$

Hence, in terms of **BCFW on-shell diagrams**,

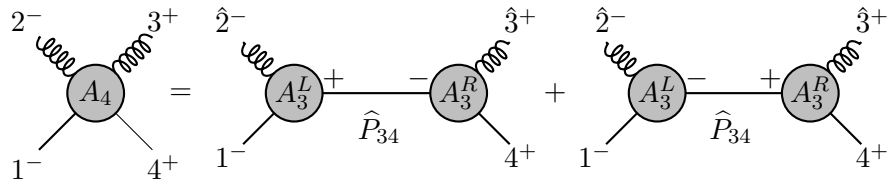

Figure 3.2: Diagrammatic representation of the BCFW recursion for qgqg process.

which can be mathematically expressed as:

$$A_4[1^-,2^-,3^+,4^+] = A_3^L[1^-,\hat{2}^-,\hat{P}_{34}^+]\frac{1}{P_{34}^2}A_3^R[-\hat{P}_{34}^-,\hat{3}^+,4^+]. \tag{3.1.2}$$

Note that the internal momentum $\widehat{P}_{34}$ is on-shell. The second diagram on the right hand-side vanishes and does not contribute to the calculation. Indeed, amplitudes with all the particles having the same helicity vanish $A_3^L[1^-,\hat{2}^-,-\widehat{P}_{34}^-] = A_3^R[-\widehat{P}_{34}^+,\hat{3}^+,4^+] = 0$. Thus, one only has to evaluate the first diagram on the left side. The first term in the Equation (3.1.2) can be computed as:

$$A_3^L[1^-,\hat{2}^-,\widehat{P}_{34}^+] = \quad = \frac{1}{\sqrt{2}}\langle 1|\gamma^\mu|\widehat{P}_{34}]\,\epsilon_\mu^-(\hat{2},k) = -\frac{\langle 1\hat{2}\rangle[k\widehat{P}_{34}]}{[k\hat{2}]}. \tag{3.1.3}$$

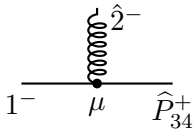

To get the final expression in this equation we used the definition of the polarization and the *Fierz rearrangement* $\langle i|\gamma^\mu|j][k|\gamma^\mu|l\rangle = 2\langle il\rangle[kj]$. To get rid of the reference momentum k, we can consider the conservation of momentum,

$$\widehat{P}_{34} = p_1 + \widehat{p}_2, \text{ implies that } \widehat{p}_2 = \widehat{P}_{34} - p_1. \tag{3.1.4}$$

By considering the following quantity:

$$[k\hat{2}]\langle\hat{2}1\rangle = [k|\widehat{p}_2|1\rangle = [k|\widehat{P}_{34} - p_1|1\rangle = [k|\widehat{P}_{34}|1\rangle = [k\widehat{P}_{34}]\langle\widehat{P}_{34}1\rangle, \tag{3.1.5}$$

and multiplying the numerator and the denominator of the equation (3.1.3) by $\langle\hat{2}1\rangle$, we get the first term of the color-ordered subamplitude:

$$A_3^L[1^-,\hat{2}^-,\widehat{P}_{34}^+] = \frac{\langle 12\rangle^2}{\langle\widehat{P}_{34}1\rangle}. \tag{3.1.6}$$

Similar approaches can be taken to evaluate the last term in (3.1.2),

$$A_3^R[-\widehat{P}_{34}^-,\hat{3}^+,4^+] = \quad = \frac{1}{\sqrt{2}}\langle -\widehat{P}_{34}|\gamma^\nu|4]\,\epsilon_\nu^+(\hat{3},r) = \frac{\langle -\widehat{P}_{34}r\rangle[\hat{3}4]}{\langle r\hat{3}\rangle}. \tag{3.1.7}$$

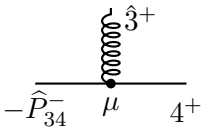

Using the momentum conservation we find $\widehat{P}_{34} = -(\widehat{p}_3 + p_4)$. This relation implies that we can express the shift-momenta $\hat{3}$ in terms of the internal momentum $\widehat{P}_{34}$ and the momentum of the outgoing quark. In order to get rid of the momentum reference r, let us compute the quantity $[4\hat{3}]\langle\hat{3}r\rangle$,

$$[4\hat{3}]\langle\hat{3}r\rangle = [4|\widehat{p}_3|r\rangle = -[4|\widehat{P}_{34} - p_4|r\rangle = -[4|\widehat{P}_{34}|r\rangle = -[4\widehat{P}_{34}]\langle\widehat{P}_{34}r\rangle, \tag{3.1.8}$$

where we used the fact that $[4|p_4|r\rangle = 0$. To satisfy analytical continuation we shall consider $\langle -\widehat{P}_{34}| = -\langle\widehat{P}_{34}|$ and $[-\widehat{P}_{34}| = [\widehat{P}_{34}|$. Taking Equation (3.1.7) and multiplying both the numerator and the denominator by $[4\hat{3}]$, we get the following expression:

$$A_3^R[-\widehat{P}_{34}^-,\hat{3}^+,4^+] = \frac{[43]^2}{[4\widehat{P}_{34}]}. \tag{3.1.9}$$

Therefore, the color-ordered amplitude $A_4[1^-,2^-,3^+,4^+]$ is given by:

$$A_4[1^-,2^-,3^+,4^+] = \frac{\langle 12\rangle^2}{\langle\widehat{P}_{34}1\rangle}\frac{1}{\widehat{P}_{34}^2}\frac{[34]^2}{[4\widehat{P}_{34}]}. \tag{3.1.10}$$

We do not want an expression of the color-ordered amplitude as a function of the internal momentum. Recall that the conservation of momentum implies that $\widehat{P}_{34} = \widehat{p}_3 + p_4$, but since the internal momentum is *on-shell* ($\widehat{P}_{34}^2 = 0$), thus $(\widehat{p}_3 + p_4)^2 = 0$. In other words, we have $\langle\hat{3}4\rangle[\hat{3}4] = 0$. However, due to the fact that $|\hat{3}]$ is not shifted, $[\hat{3}4]$ must be zero. Using the shift relation in (3.1.1),

$$\langle\hat{3}4\rangle = \langle 34\rangle - z\langle 24\rangle = 0 \Longleftrightarrow z = \frac{\langle 34\rangle}{\langle 24\rangle}. \tag{3.1.11}$$

As a consequence, the shift-equation (3.1.1) becomes:

$$|\hat{2}] = |2] + \frac{\langle 34\rangle}{\langle 24\rangle}|3], \quad |\hat{2}\rangle = |2\rangle, \tag{3.1.12}$$

$$|\hat{3}\rangle = |3\rangle - \frac{\langle 34\rangle}{\langle 24\rangle}|2\rangle, \quad |\hat{3}] = |3]. \tag{3.1.13}$$

On the other hand, we know that $|\hat{3}\rangle$ and $|4\rangle$ are two vectors in $\mathbb{C}^2$ and saying that their cross product vanishes means that $|\hat{3}\rangle$ and $|4\rangle$ have to be collinear. Consequently, $|\hat{3}\rangle$ is proportional to $|4\rangle$, so we can write $|\hat{3}\rangle = x|4\rangle$. Equating this relation to the first equation in (3.1.13), we get:

$$|3\rangle - \frac{\langle 34\rangle}{\langle 24\rangle}|2\rangle = x|4\rangle. \tag{3.1.14}$$

Here, one has the choice to multiply the equation by any vector. However, note that multiplying both sides of this equation by $\langle 2|$ will imply that $\langle 2|2\rangle = 0$, so x is given by,

$$x = \frac{\langle 23\rangle}{\langle 24\rangle}. \tag{3.1.15}$$

In terms of the square and angle brackets of $\hat{3}$ and 4, the internal momentum can be written as $\hat{P}_{34} = |\hat{3}\rangle[\hat{3}| + |4\rangle[4|$. And using the fact that $|\hat{3}\rangle$ and $|4\rangle$ are collinear, we get:

$$\widehat{P}_{34} = |4\rangle\left(\frac{\langle 23\rangle}{\langle 24\rangle}[3| + [4|\right), \tag{3.1.16}$$

which is in the form of $\widehat{P}_{34} = |\widehat{P}_{34}\rangle[\widehat{P}_{34}|$. Using the above expression, we can now derive the expression of the partial amplitude $A_4[1^-, 2^-, 3^+, 4^+]$ which is given by

$$A_4[1^-, 2^-, 3^+, 4^+] = \frac{\langle 12\rangle^3\langle 42\rangle}{\langle 12\rangle\langle 23\rangle\langle 34\rangle\langle 41\rangle}. \tag{3.1.17}$$

This is known as the Parke-Taylor formula for MHV amplitudes with 2 fermions and 2 external gluons. This formula can be generalized to n external leg of gluons using the BCFW on-shell recursion as we will show in the section 3.3.

3.2 Cross section of the process

Let us now compute the cross section of the process above, since it is the physical observable that one can measure experimentally. In order to get the cross section we have to compute the amplitude $\mathcal{A}_4$ for our helicity choice, average over the colors, and then sum over all the possible helicities.

Let us first evaluate the other partial amplitude of the form $A_4[1^-, 3^+, 2^-, 4^+]$. To get this amplitude one has to swap the two gluons in the denominator. Thus, our full amplitude is in the form of

$$\mathcal{A}_4(1^-, 2^-, 3^+, 4^+) = g_s^2 \left[T^{a_1} T^{a_2} \frac{\langle 12\rangle^3 \langle 42\rangle}{\langle 12\rangle\langle 23\rangle\langle 34\rangle\langle 41\rangle} + T^{a_2} T^{a_1} \frac{\langle 12\rangle^3 \langle 42\rangle}{\langle 13\rangle\langle 32\rangle\langle 24\rangle\langle 41\rangle} \right]. \tag{3.2.1}$$

In order to compute the cross section one has to square this expression, sum over final helicities and colors, and average over the initial helicity and color. Let us call

$$A_{4,1} = \frac{\langle 12\rangle^3 \langle 42\rangle}{\langle 12\rangle\langle 23\rangle\langle 34\rangle\langle 41\rangle} \quad \text{and} \quad A_{4,2} = \frac{\langle 12\rangle^3 \langle 42\rangle}{\langle 13\rangle\langle 32\rangle\langle 24\rangle\langle 41\rangle}. \tag{3.2.2}$$

After computing the partial amplitudes, we have to calculate the amplitude squared, and take the trace over the colors. Let us denote $\mathcal{A}_4^{-+} = \mathcal{A}_4(1^-, 2^-, 3^+, 4^+)$ where the superscript $-$ and $+$ relates the helicity of the gluon 2 and 3 respectively. We will motivate the choice of such notation later. Summing over the initial and final colors, the expression in (3.2.1) now becomes

$$\sum_{col.} |\mathcal{A}_4^{-+}|^2 = g_s^4 \left[Tr(T^{a_1} T^{a_2} T^{a_2} T^{a_1})(|A_{4,1}|^2 + |A_{4,2}|^2) + Tr(T^{a_1} T^{a_2} T^{a_1} T^{a_2})(A_{4,1}^* A_{4,2} + A_{4,1} A_{4,2}^*) \right].$$

In matrix notation, the trace of the matrix generators can be written as:

$$Tr(T^{a_1} T^{a_2} T^{a_2} T^{a_1}) = (T^{a_1})_{ij} (T^{a_1})_{jk} (T^{a_2})_{kl} (T^{a_2})_{li}, \tag{3.2.3}$$

$$Tr(T^{a_1} T^{a_2} T^{a_1} T^{a_2}) = (T^{a_1})_{ij} (T^{a_1})_{kl} (T^{a_2})_{jk} (T^{a_2})_{li}. \tag{3.2.4}$$

Using the relation given in (2.1.2) and taking into account the property of the Kronecker delta, for instance $\delta_{ii} = N$, the trace in 3.2.3 can be evaluated as

$$Tr(T^{a_1} T^{a_2} T^{a_2} T^{a_1}) = \left(\delta_{ik}\delta_{jj} - \frac{1}{N}\delta_{ij}\delta_{jk} \right) \left(\delta_{ki}\delta_{ll} - \frac{1}{N}\delta_{kl}\delta_{li} \right) = \delta_{ik}\delta_{ki} \left(\frac{N^2-1}{N} \right)^2 = N \left(\frac{N^2-1}{N} \right)^2.$$

By taking a similar approach, the second trace term (3.2.4) gives

$$Tr(T^{a_1} T^{a_2} T^{a_1} T^{a_2}) = (T^{a_2})_{jk} (T^{a_2})_{li} \left[\delta_{il}\delta_{jk} - \frac{1}{N}\delta_{ij}\delta_{kl} \right] = -\left(\frac{N^2-1}{N} \right),$$

where in the last step we expand the relation and used the fact that $(T^{a_2})_{kk}(T^{a_2})_{ll} = 0$. The remaining term $(T^{a_2})_{ik}(T^{a_2})_{ki}$ was evaluated using the previous result from the computation of the first trace. To simplify notation, we can write the traces in the form:

$$Tr(T^{a_1} T^{a_2} T^{a_2} T^{a_1}) = C_A C_F^2 \quad \text{and} \quad Tr(T^{a_1} T^{a_2} T^{a_1} T^{a_2}) = -C_F, \tag{3.2.5}$$

where

$$C_A = N \quad \text{and} \quad C_F = \frac{N^2-1}{N}. \tag{3.2.6}$$

The square of the partial amplitudes and the crossed terms can be expressed in terms of the **Mandelstam variables** s, u and t introduced earlier. Recalling the Lorentz invariant product s_{ij}, which are defined as $s_{ij} = \langle ij\rangle[ij]$, we have

$$|A_{4,1}|^2 = A_{4,1} A_{4,1}^* = \left(\frac{\langle 12\rangle^3 \langle 42\rangle}{\langle 12\rangle\langle 23\rangle\langle 34\rangle\langle 41\rangle} \right) \left(\frac{[12]^3 [42]}{[12][23][34][41]} \right) = \frac{s_{12}\, s_{13}}{s_{14}^2} = \frac{tu}{s^2}, \tag{3.2.7}$$

$$|A_{4,2}|^2 = A_{4,2} A_{4,2}^* = \left(\frac{\langle 12\rangle^3 \langle 42\rangle}{\langle 13\rangle\langle 32\rangle\langle 24\rangle\langle 41\rangle} \right) \left(\frac{[12]^3 [42]}{[13][32][24][41]} \right) = \frac{s_{12}^3}{s_{13}\, s_{14}} = \frac{t^3}{us}. \tag{3.2.8}$$

The computation of the crossed term is a little trickier. If a spinor appears in a physical quantity, then it must terminate, i.e. it has the form $\langle i_1 i_2\rangle[i_2 i_3]\cdots[i_n i_1]$. Using short-hand notation, we write $\langle i_1\cdots i_n i_1]$. Such a quantity can be evaluated by performing Dirac traces. For instance,

$$\begin{aligned}\langle ij\rangle[jk]\langle kl\rangle[li] &= \frac{1}{2}\left[Tr(1-\gamma_5)\not{p}_i\not{p}_j\not{p}_k\not{p}_l\right]\\ &= \frac{1}{2}\left[s_{ij}s_{kl}+s_{il}s_{jk}-s_{ik}s_{jl}-4i\varepsilon(i,j,k,l)\right],\end{aligned} \tag{3.2.9}$$

where $\varepsilon(i,j,k,l)=\varepsilon_{\mu\nu\rho\sigma}p_i^\mu p_j^\nu p_k^\rho p_l^\sigma$ and $\varepsilon_{\mu\nu\rho\sigma}$ is the completely antisymmetric tensor. Using these tools, the crossed term in the square amplitude can be written as

$$\begin{aligned}A^*_{4,1}A_{4,2}+A_{4,1}A^*_{4,2} &= -\frac{t^3u}{s^2}\left[\frac{1}{\langle 13\rangle[34]\langle 42\rangle[21]}+\frac{1}{[13]\langle 34\rangle[42]\langle 21\rangle}\right]\\ &= -\frac{t^3u}{s^2}\left[\frac{1}{\langle 13421]}+\frac{1}{\langle 12431]}\right].\end{aligned} \tag{3.2.10}$$

Using the formula in (3.2.9), the terms in the denominators give:

$$\langle 13421] = \frac{1}{2}(t^2+u^2-s^2)-2i\varepsilon_{\mu\nu\rho\sigma}p_1^\mu p_3^\nu p_4^\rho p_2^\sigma, \tag{3.2.11}$$

$$\langle 12431] = \frac{1}{2}(t^2+u^2-s^2)-2i\varepsilon_{\mu\nu\rho\sigma}p_1^\mu p_2^\nu p_4^\rho p_3^\sigma. \tag{3.2.12}$$

Since the $\varepsilon_{\mu\nu\rho\sigma}$ is antisymmetric, swapping two indices will give rise to a minus sign. It is straightforward to see that $\langle 13421] = \langle 12431]^*$. Therefore, the equation (3.2.10) now becomes:

$$A^*_{4,1}A_{4,2}+A_{4,1}A^*_{4,2} = -\frac{t^3u}{s^2}\cdot\frac{2\mathfrak{Re}(\langle 13421])}{|\langle 13421]|^2}, \tag{3.2.13}$$

where $|\langle 13421]|^2 = |\langle 13\rangle[34]\langle 42\rangle[21]|^2 = u^2s^2$. Rearranging the expression and by doing some simplifications, we get the crossed term:

$$A^*_{4,1}A_{4,2}+A_{4,1}A^*_{4,2} = -\frac{t}{us^2}(t^2+u^2-s^2). \tag{3.2.14}$$

For QCD, the gauge group is $SU(3)$, where the color-indices run over $a_1, a_2, \cdots = 1,\cdots,8$. Thus, to dos the color average, we have to set $N=3$. By combining all the results from the previous calculations, we can now write down the expression of the square amplitude as

$$\begin{aligned}\sum_{col.}|\mathcal{A}_4^{-+}|^2 &= g_s^4\left[\frac{64}{3}\frac{t}{us^2}(u^2+t^2)+\frac{8}{3}\frac{t}{us^2}(t^2+u^2-s^2)\right]\\ &= g_s^4\left[\frac{72}{3}\frac{t}{us^2}(u^2+t^2)-\frac{8}{3}\frac{t}{u}\right]\end{aligned} \tag{3.2.15}$$

Recalling the property of the Mandelstam variables for massless particles, $s+u+t=0$, we can write $u^2+t^2=(u+t)^2-2ut=s^2-2ut$. Finally, we get the expression:

$$\sum_{col.}|\mathcal{A}_4^{-+}|^2 = \frac{64}{3}g_s^4\left[\frac{u}{t}-\frac{9}{4}\frac{t^2}{s^2}\right]. \tag{3.2.16}$$

The last result represents the square of the amplitude averaged over the colors for the helicity choice $(-,-,+,+)$. Let us now find the full amplitude squared by taking into account all the possible

helicities. For the process $q\bar{q}gg$, there are 4 possibles configurations for non-vanishing amplitude: $(-,-,+,+),(-,+,-,+),(+,-,+,-)$ and $(+,+,-,-)$. However, due to the Parity of the MHV-partial amplitudes,

$$|\mathcal{A}_4(1^-,2^-,3^+,4^+)|^2 = |\mathcal{A}_4(1^+,2^+,3^-,4^-)|^2 \tag{3.2.17}$$
$$|\mathcal{A}_4(1^-,2^+,3^-,4^+)|^2 = |\mathcal{A}_4(1^+,2^-,3^+,4^-)|^2 \tag{3.2.18}$$

That is to say, we do not have to take into consideration the helicity of the quarks while doing the average. Hence, we only have to compute $\sum_{col.}|\mathcal{A}_4^{-+}|^2$ and $\sum_{col.}|\mathcal{A}_4^{+-}|^2$. However, flipping helicity of two gluons is equivalent to swapping the gluons, in this case $1 \leftrightarrow 2$ $(s_{12} \leftrightarrow s_{13})$,

$$\sum_{hel.}\sum_{col.}\mathcal{A}_4 = \sum_{col.}(|\mathcal{A}_4^{-+}|^2 + |\mathcal{A}_4^{+-}|^2) = \frac{64}{3}g_s^4\left[\frac{u}{t} - \frac{9}{4}\frac{t^2}{s^2} + \frac{t}{u} - \frac{9}{4}\frac{u^2}{s^2}\right]. \tag{3.2.19}$$

To get the full expression of the cross section, we must add the factors for averaging over the initial colors and helicities. Therefore, the final expression of the cross section of the $q\bar{q}gg$ process is given by

$$\frac{d\sigma}{d\cos\theta}(q\bar{q}\to gg) = \frac{16}{27}\frac{\pi\alpha_s^2}{s}\left[\frac{u^2+t^2}{ut} - \frac{9}{4}\frac{u^2+t^2}{s^2}\right], \tag{3.2.20}$$

where θ is the scattering angle and s is the square of the center of mass energy. To get the $qg\to qg$ channel, we apply the crossing symmetry rules, thus

$$\frac{d\sigma}{d\cos\theta}(qg\to qg) = \frac{2}{9}\frac{\pi\alpha_s^2}{s}\left[\frac{9}{4}\frac{u^2+s^2}{t^2} - \frac{u^2+t^2}{us}\right]. \tag{3.2.21}$$

The last result represents the differential cross section of process $qg\to qg$. This is consistent with the expression of cross section in Trivedi et al. (2014).

3.3 Generalization of the partial amplitude formula

For a 4-point amplitude, the Parke-Taylor formula for the MHV-amplitude is given by Equation (3.1.17). Let us now recover the Parke-Taylor formula for $(n+2)$-point amplitude, with a quark-antiquark pair and n gluons, by induction. For the choice of helicity we can choose the quark p and the gluon 1 to have a negative helicity which forces the remaining particles to have a positive helicity. By considering a $[1,2\rangle$-shift we can show that the only non-vanishing BCFW diagram is given by the Figure 3.3. One

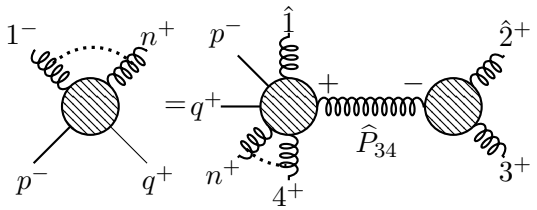

Figure 3.3: BCFW diagram for the A_{n+2} MHV-amplitude.

can check that the subdiagram on the left has $(n-1)$ legs, while the subdiagram in the right has 3 legs. For the $[1,2\rangle$-shift, the momentum are deformed as follows,

$$|\hat{1}] = |1] + z|2],\ |\hat{1}\rangle = |1\rangle \quad \text{and} \quad |\hat{2}\rangle = |2\rangle - z|1\rangle,\ |\hat{2}] = |2]. \tag{3.3.1}$$

We showed that for a process which involves 4 external particles, the Parke-Taylor formula is true. Assuming that the Parke-Taylor formula is true for $(n-1)$-point amplitude, the subdiagram on the left is given by

$$A_{n-1}[p^-, \hat{1}^-, \widehat{P}_{23}^+, ..., n^+, q^+] = \frac{\langle p\hat{1}\rangle^3\langle q\hat{1}\rangle}{\langle p\hat{1}\rangle\langle \hat{1}\widehat{P}_{23}\rangle\langle\widehat{P}_{23}4\rangle\cdots\langle nq\rangle\langle qp\rangle}. \tag{3.3.2}$$

To get the full expression of the $(n+2)$ color-ordered partial amplitudes we need to evaluate the subdiagram on the right. The 3-point amplitude for pure gluons can be computed using the spinor helicity. So, let us evaluate the following 3-gluon process:

$A_3[1^-, 2^+, 3^+] =$ 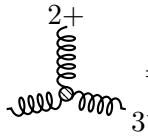

$= \epsilon^-(1,r)\epsilon^+(2,k)(p_1-p_2)\epsilon^+(3,s) + \epsilon^+(2,k)\epsilon^+(3,s)(p_2-p_3)$
$\epsilon^-(1,r) + \epsilon^+(3,s)\epsilon^-(1,r)(p_3-p_1)\epsilon^+(2,k).$

Let us choose the reference momentum of the gluon 3 in a such way that $\epsilon^+(2,k)\epsilon^+(3,s) = 0$, which means that $k \equiv s$. So our polarization vectors are defined as follows:

$$\epsilon_\mu^-(1,r) = -\frac{1}{\sqrt{2}}\frac{[r|\gamma_\mu|1\rangle}{[1r]}, \quad \epsilon_\mu^+(2,s) = \frac{1}{\sqrt{2}}\frac{[2|\gamma_\mu|s\rangle}{\langle s2\rangle}, \quad \text{and} \quad \epsilon_\mu^+(3,s) = \frac{1}{\sqrt{2}}\frac{[3|\gamma_\mu|s\rangle}{\langle s3\rangle}. \tag{3.3.3}$$

Using the property of the angle-square bracket, we get the following expression,

$$A_3[1^-, 2^+, 3^+] = \frac{\langle 1s\rangle[r2][3|p_1-p_2|s\rangle + \langle 1s\rangle[r3][2|p_3-p_1|3\rangle}{[1r]\langle s2\rangle\langle s3\rangle}. \tag{3.3.4}$$

By developing the remaining angle-square bracket expression, and by doing some simplifications, we get the following expression:

$$A_3[1^-, 2^+, 3^+] = \frac{\langle 1s\rangle^2}{[1r]\langle s2\rangle\langle s3\rangle}\left([r2][31] - [r3][21]\right). \tag{3.3.5}$$

We can see that the term in the bracket can be rewritten in terms of the Schouten identity,

$$[r2][31] - [r3][21] = [r1][32]. \tag{3.3.6}$$

Hence, the expression of the amplitude of the 3-gluons process now becomes,

$$A_3[1^-, 2^+, 3^+] = \frac{\langle 1s\rangle^2[23]}{\langle s2\rangle\langle s3\rangle}. \tag{3.3.7}$$

We want to get rid of the momentum reference s and to have an expression which only depends on square or angle brackets. By multiplying the numerator and the denominator by $[23]^2$ and rearranging the term in the denominator, the factor $\langle 1s\rangle$ cancels, and we get

$$A_3[1^-, 2^+, 3^+] = \frac{[23]^4}{[12][23][31]}. \tag{3.3.8}$$

Thus, for a pure gluon process defined by $A_3[-\widehat{P}_{23}^-, \hat{2}^+, 3^+]$, the 3-point amplitude is given by,

$$A_3[-\widehat{P}_{23}^-, \hat{2}^+, 3^+] = \frac{[\hat{2}3]}{[-\widehat{P}_{23}\hat{2}][\hat{2}3][-3\widehat{P}_{23}]}. \tag{3.3.9}$$

The color-ordered amplitude A_{n+2} can be therefore written as,

$$A_{n+2}[p^-,1^-,2^+,\cdots,n^+,q^+] = \frac{\langle p\hat{1}\rangle^3\langle q\hat{1}\rangle}{\langle p\hat{1}\rangle\langle\hat{1}\widehat{P}_{23}\rangle\langle\widehat{P}_{23}4\rangle\cdots\langle nq\rangle\langle qp\rangle}\frac{1}{\langle 23\rangle[23]}\frac{[\hat{2}3]}{[-\widehat{P}_{23}^-\hat{2}][\hat{2}3][-3\widehat{P}_{23}^-]}. \quad (3.3.10)$$

We can compute the angle and the square brackets of the shifted momenta $\widehat{P}_{23}$ as we did previously for the 4-point amplitude. However, by considering the property $\langle ij\rangle[jk] = \langle i|j|k]$ we can combine the terms in the denominator containing the shifted momenta. Combining the factors from the denominator,

$$\langle 1\widehat{P}_{23}\rangle[3\widehat{P}_{23}^-] = -\langle 1|\widehat{p}_2 + p_3|3] = -\langle\hat{1}\hat{2}\rangle[\hat{2}3], \quad (3.3.11)$$

$$\langle\widehat{P}_{23}^-4\rangle[\widehat{P}_{23}^-2] = -\langle 3|\widehat{p}_2 + p_3|\hat{2}] = -\langle 34\rangle[\hat{2}3]. \quad (3.3.12)$$

Note that for analytical continuity we considered $\langle -\widehat{P}_{23}| = -\langle\widehat{P}_{23}|$ and $[-\widehat{P}_{23}| = [\widehat{P}_{23}|$. Also, since $|\hat{1}\rangle, |\hat{2}]$ and $\langle\hat{1}\hat{2}\rangle$ remain unshifted, the final expression of A_{n+1} is given by,

$$A_{n+2}[p^-,1^-,2^+,\cdots,n^+,q^+] = \frac{\langle p1\rangle^3\langle q1\rangle}{\langle p1\rangle\langle 12\rangle\cdots\langle nq\rangle\langle qp\rangle}. \quad (3.3.13)$$

This is the general formula for a MHV-amplitude with a pair of quark anti-quark and n external gluons. This formula will be used later in our calculations, when we compute the process $qg \to qg + ng$, where $n = 1, 2$.

4. Process with emission of radiation

In heavy-ion collisions there is evidence of jet production. When these jets propagate through a medium, energy losses are expected. Indeed, the interaction between a high energy quark and a thermal gluon can yield the emission of radiative gluons and the decrease of the energy of the quark. The information about these radiative gluons near the soft and collinear limit is encoded in the so called *soft collinear factor*. Considering the process $qg \to qg$, where we have $n-2$ Bremsstrahlung gluons, we want to show that at the soft collinear limit the full amplitude factorizes as

$$\mathcal{A}(p, k_1, k_2; k_3, \cdots, k_n; q) \longrightarrow \mathcal{A}(p, k_1, k_2, q) J(k_3, \cdots, k_n). \tag{4.0.1}$$

Here J is the *soft collinear factor*, also known as radiative gluon bremsstrahlung. In order to get the energy loss in a QGP, one has to evaluate first the distribution of the radiative gluons emanating from the outgoing quark, which is given by the summation of the radiative term J at the cross section level. In the literature, the momentum distribution of the radiative gluons has been approximated to the *Poisson Convolution*, which assumes that the emission of gluons are independent,

$$dN^{(n)} \longrightarrow g_s^{2n} \frac{C_F^n}{n!} \prod_{i=1}^{n} \frac{dx_i}{x_i} \frac{dk_{i_\perp}^2}{k_{i_\perp}^2}, \tag{4.0.2}$$

where $k_{i_\perp}$ is the transverse momentum of the i^{th} radiated gluon, C_F^n and n represent respectively the color factor and the radiated gluons. In this section we will see a smooth calculation of the *soft collinear factor* and the distribution of the radiative gluons using the MHV-techniques.

4.1 Parametrization of the kinematics

By colliding heavy-ions, quarks and gluons may slam directly into each other and scatter back to back. In this problem, consider a *hard scattering* (see Figure 4.1) where we have a large momentum quark colliding with a gluon which is moving in the opposite direction. As a result of the collision, we have an outgoing quark which is perpendicular to the incoming quark. We consider the radiated gluon to be soft and collinear to the outgoing quark. We can choose the incident quark momentum to lie along the $\hat{1}$-axis and the soft gluon to lie in the $\hat{1}$-$\hat{2}$ plane of the momentum space.

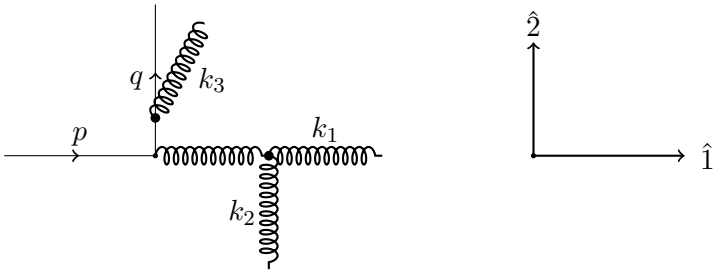

Figure 4.1: Schematic view of the kinematics of a hard scattering process.

Since the radiated gluon is set to be soft, its energy must be very small. Choosing x_3 to be the fraction of the energy of the initial quark that is carried off by the soft gluon, let us denote the usual four-momenta

with parentheses and light-cone momenta with brackets. The momentum of the incident quark is then $p = (E, E, 0, 0) = [2E, 0, \mathbf{0}]$, while the momentum of the radiated gluon is

$$k_3 = \left(x_3 E, k_{3_\perp}, \sqrt{(x_3 E)^2 - k_{3_\perp}^2}, 0\right) = \left[x_3 E + k_{3_\perp}, x_3 E - k_{3_\perp}, \left(\sqrt{(x_3 E)^2 - k_{3_\perp}^2}, 0\right)\right], \tag{4.1.1}$$

where $k_{3_\perp}$ is the transverse momentum of the radiated gluon 3. The component of k_3 along the $\hat{2}$-axis is chosen to keep $k_3^2 = 0$. Thus, the energy of the outgoing quark after energy loss is

$$q = ((1 - x_3)E, 0, (1 - x_3)E, 0) = [(1 - x_3)E, (1 - x_3)E, ((1 - x_3)E, 0)]. \tag{4.1.2}$$

Since we are considering a hard scattering, the incoming quark has to have a large momentum, thus $k_1 = (E, -E, 0, 0)$, and for completeness, the momentum of the outgoing gluon can be parametrized as $k_2 = (E, 0, -E, 0)$. These momentum satisfy the on-shell condition $p^2 = q^2 = k_1^2 = k_2^2 = k_3^2 = 0$.

Let us consider the following approximations for our parton energy loss model:

- *Eikonal trajectory*: The energy of the leading parton E is much higher than the transverse momentum $k_{3_\perp}$, $E \gg k_{3_\perp}$.
- *Small angle/collinear emission*: The energy of the emitted gluon $\omega_3 = x_3 E$ is sufficiently high compared to its transverse momentum $k_{3_\perp}$, $\omega_3 \gg k_{3_\perp}$.
- *Soft approximation*: The energy of the leading parton E is much larger than the energy of the emitted gluon ω_3, $E \gg \omega_3$.

With these approximations we can now compute the scalar product of pairs of momentum: $p \cdot q \approx E^2$, $p \cdot k_1 = 4E^2$, $p \cdot k_2 = E^2$, $k_1 \cdot k_3 \approx x_3 E^2$, $k_2 \cdot k_3 \approx 2x_3 E^2$ and $p \cdot k_3 \approx x_3 E^2$. In order to compute the scalar product of $q \cdot k_3$, let us first do the Taylor expansion of $\sqrt{(x_3 E)^2 - k_{3_\perp}^2}$.

$$\sqrt{(x_3 E)^2 - k_{3_\perp}^2} = x_3 E \left(1 - \frac{k_{3_\perp}^2}{2(x_3 E)^2}\right) + \mathcal{O}\left(\frac{k_{3_\perp}^4}{(x_3 E)^4}\right). \tag{4.1.3}$$

Thus,

$$q \cdot k_3 = x_3(1 - x_3)E^2 - x_3(1 - x_3)E^2 \left(1 - \frac{k_{3_\perp}^2}{2(x_3 E)^2}\right) \approx \frac{k_{3_\perp}^2}{2x_3}. \tag{4.1.4}$$

4.2 One Bremsstrahlung gluon

Let us now compute the process where we have an emission of a radiated gluon. From now, let us label the pair of quark anti-quark by p and q respectively and the two gluons are labeled by 1 and 2 with color indices a_1 and a_2 (see Figure 4.2).

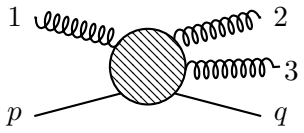

Figure 4.2: MHV-diagram for $q\bar{q}gg$-process with 1 gluon emission.

The full amplitude of this process is given by:

$$\mathcal{A}_5(p,1,2,3,q) = g_s^3 \sum_{\sigma\in S_3} T^{a_{\sigma(1)}} T^{a_{\sigma(2)}} T^{a_{\sigma(3)}} A_5[p,\sigma(1),\sigma(2),\sigma(3),q]. \tag{4.2.1}$$

Let us choose the helicity to be $(--+++)$ in order to violate the helicity. With this choice of helicity and applying the MHV-formula for the quark-gluon amplitude, we have:

$$\mathcal{A}_5(p^-,1^-,2^+,3^+,q^+) = g_s^3 \sum_{\sigma\in S_3} T^{a_{\sigma(1)}} T^{a_{\sigma(2)}} T^{a_{\sigma(3)}} \frac{\langle p1\rangle^3\langle q1\rangle}{\langle p\sigma(1)\rangle\langle\sigma(1)\sigma(2)\rangle\langle\sigma(2)\sigma(3)\rangle\langle\sigma(3)q\rangle\langle qp\rangle} \tag{4.2.2}$$

By expanding this expression we get $3! = 6$ terms, which means that we have to compute 6 different partial amplitudes. Using a similar notation as in the previous chapter, $\mathcal{A}_5^{-++} = \mathcal{A}_5(p^-,1^-,2^+,3^+,q^+)$, let us first write down the full expression of the amplitude

$$\begin{aligned}\mathcal{A}_5^{-++} = g_s^3 &\left[\frac{T^{a_1}T^{a_2}T^{a_3}\langle p1\rangle^3\langle q1\rangle}{\langle p1\rangle\langle 12\rangle\langle 23\rangle\langle 3q\rangle\langle qp\rangle} + \frac{T^{a_1}T^{a_3}T^{a_2}\langle p1\rangle^3\langle q1\rangle}{\langle p1\rangle\langle 13\rangle\langle 32\rangle\langle 2q\rangle\langle qp\rangle} + \frac{T^{a_3}T^{a_1}T^{a_2}\langle p1\rangle^3\langle q1\rangle}{\langle p3\rangle\langle 31\rangle\langle 12\rangle\langle 2q\rangle\langle qp\rangle}\right] \\ + g_s^3 &\left[\frac{T^{a_2}T^{a_1}T^{a_3}\langle p1\rangle^3\langle q1\rangle}{\langle p2\rangle\langle 21\rangle\langle 13\rangle\langle 3q\rangle\langle qp\rangle} + \frac{T^{a_2}T^{a_3}T^{a_1}\langle p1\rangle^3\langle q1\rangle}{\langle p2\rangle\langle 23\rangle\langle 31\rangle\langle 1q\rangle\langle qp\rangle} + \frac{T^{a_3}T^{a_2}T^{a_1}\langle p1\rangle^3\langle q1\rangle}{\langle p3\rangle\langle 32\rangle\langle 21\rangle\langle 1q\rangle\langle qp\rangle}\right].\end{aligned} \tag{4.2.3}$$

Taking the square of this expression will be very complicated. Indeed, squaring this amplitude will give rise to 36 non-trivial terms. Since we want to know how $\mathcal{A}_5$ is related to $\mathcal{A}_4$, it might be a good idea to express the amplitude $\mathcal{A}_5^{-++}$ in terms of $\mathcal{A}_4^{-+}$. We will then use the *soft-eikonal approximation* to simplify calculations.

If we look carefully at the partial amplitudes in $\mathcal{A}_5$, we notice that we can do a factorization on the kinematics in order to get the partial amplitudes $A_{4,1}$ and $A_{4,2}$ of $\mathcal{A}_4$. After factorization we get:

$$\begin{aligned}\mathcal{A}_5^{-++} = g_s^3 &\left[T^{a_1}T^{a_2}T^{a_3}\frac{\langle 2q\rangle}{\langle 23\rangle\langle 3q\rangle} + T^{a_1}T^{a_3}T^{a_2}\frac{\langle 12\rangle}{\langle 13\rangle\langle 32\rangle} + T^{a_3}T^{a_1}T^{a_2}\frac{\langle p1\rangle}{\langle p3\rangle\langle 31\rangle}\right] A_{4,1} \\ + g_s^3 &\left[T^{a_2}T^{a_1}T^{a_3}\frac{\langle 1q\rangle}{\langle 13\rangle\langle 3q\rangle} + T^{a_2}T^{a_3}T^{a_1}\frac{\langle 21\rangle}{\langle 23\rangle\langle 31\rangle} + T^{a_3}T^{a_2}T^{a_1}\frac{\langle p2\rangle}{\langle p3\rangle\langle 32\rangle}\right] A_{4,2}.\end{aligned} \tag{4.2.4}$$

We notice that all the partial amplitudes inside the brackets depend on the momentum of the soft gluon. Let us call these terms $S(i,3^+,j)$, where:

$$S(i,3^+,j) = \frac{\langle ij\rangle}{\langle i3\rangle\langle 3j\rangle}. \tag{4.2.5}$$

We can recognize here the general form of the *soft factor* $S(i,3^+,j)$ where the soft gluon 3 (with helicity $h_3 = -1$) is emitted between the two external legs i and j. Generally, for a process involving a soft gluon s, the color-ordered amplitude can always be factorized as

$$A[p,1,\cdots,i,s^\pm,j,\cdots,n,q] = S(i,s^\pm,j)A[p,1,\cdots,i,j,\cdots,n,q], \tag{4.2.6}$$

where

$$S(i,s^+,j) = \frac{\langle ij\rangle}{\langle is\rangle\langle sj\rangle} \quad \text{and} \quad S(i,s^-,j) = \frac{[ij]}{[is][sj]}. \tag{4.2.7}$$

Note here that the soft factor does not depend on the helicity of i and j and $|S(i,s^-,j)|^2 = |S(i,s^+,j)|^2$. In order to get the expression of the amplitude $\mathcal{A}_4$, we have to deal with the color terms. Using the

normalization and the definition of the structure constants in section 2.1, we can transform the product of the generator matrices in $\mathcal{A}_5$ (4.2.4) as follows:

$$T^{a_1}T^{a_3}T^{a_2} = T^{a_1}T^{a_2}T^{a_3} + i\tilde{f}^{a_3a_2c}T^{a_1}T^{c}, \tag{4.2.8}$$

$$T^{a_3}T^{a_1}T^{a_2} = T^{a_1}T^{a_2}T^{a_3} + i\tilde{f}^{a_3a_1c}T^{a_1}T^{c} + i\tilde{f}^{a_3a_1c}T^{c}T^{a_2}. \tag{4.2.9}$$

We can get the remaining terms by permuting a_1 and a_2. By virtue of these transformations, the amplitude in (4.2.4) can be written as

$$\begin{aligned}\mathcal{A}_5^{-++} =& g_s^3\, T^{a_1}T^{a_2}A_{4,1}\left[T^{a_3}\frac{\langle 2q\rangle}{\langle 23\rangle\langle 3q\rangle} + T^{a_3}\frac{\langle 12\rangle}{\langle 13\rangle\langle 32\rangle} + T^{a_3}\frac{\langle p1\rangle}{\langle p3\rangle\langle 31\rangle}\right] + \\ & g_s^3\, T^{a_2}T^{a_1}A_{4,2}\left[T^{a_3}\frac{\langle 1q\rangle}{\langle 13\rangle\langle 3q\rangle} + T^{a_3}\frac{\langle 21\rangle}{\langle 23\rangle\langle 31\rangle} + T^{a_3}\frac{\langle p2\rangle}{\langle p3\rangle\langle 32\rangle}\right] + \\ & ig_s^3\, A_{4,1}\left[\tilde{f}^{a_3a_2c}T^{a_1}T^{c}\left(\frac{\langle p1\rangle}{\langle p3\rangle\langle 31\rangle} + \frac{\langle 12\rangle}{\langle 13\rangle\langle 32\rangle}\right) + \tilde{f}^{a_3a_1c}T^{c}T^{a_2}\frac{\langle p1\rangle}{\langle p3\rangle\langle 31\rangle}\right] + \\ & ig_s^3\, A_{4,2}\left[\tilde{f}^{a_3a_1c}T^{a_2}T^{c}\left(\frac{\langle p2\rangle}{\langle p3\rangle\langle 32\rangle} + \frac{\langle 21\rangle}{\langle 23\rangle\langle 31\rangle}\right) + \tilde{f}^{a_3a_2c}T^{c}T^{a_1}\frac{\langle p2\rangle}{\langle p3\rangle\langle 32\rangle}\right].\end{aligned} \tag{4.2.10}$$

This expression can be simplified using the *Schouten identity* (Witten, 2004), which is defined as

$$\langle ij\rangle\langle sk\rangle + \langle si\rangle\langle jk\rangle + \langle sj\rangle\langle ki\rangle = 0. \tag{4.2.11}$$

Let us consider two soft partial amplitudes $S(i,s,j)$ and $S(j,s,k)$ defined as in (4.2.5), then

$$S(i,s^+,j) + S(j,s^+,k) = \frac{\langle ij\rangle}{\langle is\rangle\langle sj\rangle} + \frac{\langle jk\rangle}{\langle js\rangle\langle sk\rangle} = \frac{\langle js\rangle\left(\langle ij\rangle\langle sk\rangle - \langle is\rangle\langle jk\rangle\right)}{\langle js\rangle^2\langle is\rangle\langle ks\rangle}. \tag{4.2.12}$$

And by applying the *Schouten identity* (4.2.11), we get

$$S(i,s^+,j) + S(j,s^+,k) = \frac{\langle ik\rangle}{\langle is\rangle\langle sk\rangle}. \tag{4.2.13}$$

It follows from this calculation that $S(i_1,s,i_2) + S(i_2,s,i_3) + \cdots + S(i_{n-1},s,i_n) = S(i_1,s,i_n)$. Armed with this simplification, the expression of the amplitude in (4.2.10) now becomes

$$\begin{aligned}\mathcal{A}_5^{-++} =& g_s^3\,\left(T^{a_1}T^{a_2}A_{4,1} + T^{a_2}T^{a_1}A_{4,2}\right)\left[T^{a_3}\frac{\langle pq\rangle}{\langle p3\rangle\langle 3q\rangle}\right] + ig_s^3\, A_{4,1}\left[\tilde{f}^{a_3a_2c}T^{a_1}T^{c}\frac{\langle p2\rangle}{\langle p3\rangle\langle 32\rangle} + \right. \\ & \left. \tilde{f}^{a_3a_1c}T^{c}T^{a_2}\frac{\langle p1\rangle}{\langle p3\rangle\langle 31\rangle}\right] + ig_s^3\, A_{4,2}\left[\tilde{f}^{a_3a_1c}T^{a_2}T^{c}\frac{\langle p1\rangle}{\langle p3\rangle\langle 31\rangle} + \tilde{f}^{a_3a_2c}T^{c}T^{a_1}\frac{\langle p2\rangle}{\langle p3\rangle\langle 32\rangle}\right].\end{aligned} \tag{4.2.14}$$

Note that in the first term of this expression appears the amplitude $\mathcal{A}_4^{-+}$ for the 4-process. Hence, we can rewrite this equation as

$$\begin{aligned}\mathcal{A}_5^{-++} = g_s\,\mathcal{A}_4^{-+}\left[T^{a_3}\frac{\langle pq\rangle}{\langle p3\rangle\langle 3q\rangle}\right] &+ ig_s^3\frac{\langle p2\rangle}{\langle p3\rangle\langle 32\rangle}\left[\tilde{f}^{a_3a_2c}T^{a_1}T^{c}A_{4,1} + \tilde{f}^{a_3a_2c}T^{c}T^{a_1}A_{4,2}\right] \\ &+ ig_s^3\frac{\langle p1\rangle}{\langle p3\rangle\langle 31\rangle}\left[\tilde{f}^{a_3a_1c}T^{a_2}T^{c}A_{4,2} + \tilde{f}^{a_3a_1c}T^{c}T^{a_2}A_{4,1}\right]\end{aligned} \tag{4.2.15}$$

This expression looks much better than the expression in (4.2.3), where we have 6 partial amplitudes contributing to the full amplitude. Still, when we take the square of this expression it will not be an

easy task. Fortunately, with the *soft-eikonal approximation*, we can neglect the last two terms. Based on our parametrization in the previous section $\langle pq\rangle, \langle p1\rangle, \langle p2\rangle$ are in the order of E^2, $\langle p3\rangle, \langle 31\rangle, \langle 32\rangle$ are of order of x_3E^2 while $\langle q3\rangle$ is of the order of $k_{3_\perp}^2/x_3$. Because of the *eikonal approximation*, the transverse momentum of the radiated gluon is much smaller than its energy, so $k_{3_\perp}^2 << (x_3E)^2$.

Thus, the amplitude for the $q\bar{q}gg$-process with an emission of radiated gluon is given by

$$\mathcal{A}_5^{-++} \approx g_s\, \mathcal{A}_4^{-+} \left[T^{a_3} \frac{\langle pq\rangle}{\langle p3\rangle\langle 3q\rangle}\right]. \tag{4.2.16}$$

Taking the square of this amplitude and averaging over the initial colors and helicities, gives the following result,

$$\sum_{col.} |\mathcal{A}_5^{-++}|^2 \approx g_s^2 Tr(T^{a_3}T^{a_3}|\mathcal{A}_4^{-+}|^2) \left|\frac{\langle pq\rangle}{\langle p3\rangle\langle 3q\rangle}\right|^2. \tag{4.2.17}$$

The trace can be evaluated as

$$Tr(T^{a_3}T^{a_3}|\mathcal{A}_4^{-+}|^2) = (T^{a_3})_{ij}(T^{a_3})_{jk}|\mathcal{A}_4^{-+}|^2_{ki} = (T^{a_3}T^{a_3})_{ik}|\mathcal{A}_4^{-+}|^2_{ki} = C_F\delta_{ik}|\mathcal{A}_4^{-+}|^2_{ki}, \tag{4.2.18}$$

which tells us that $Tr(T^{a_3}T^{a_3}|\mathcal{A}_4^{-+}|^2) = C_F Tr(|\mathcal{A}_4^{-+}|^2)$. We can now plug this relation into (4.2.17) to get the final answer of the amplitudes:

$$\sum_{col.} |\mathcal{A}_5^{-++}|^2 \approx g_s^2 C_F \frac{(p\cdot q)}{(k_3\cdot p)(k_3\cdot q)} \sum_{col.} |\mathcal{A}_4^{-+}|^2. \tag{4.2.19}$$

Now, consider all the possible configurations of helicity. By virtue of the soft factorization in (4.2.6), and the *soft-eikonal approximation* we have the following factorization,

$$\mathcal{A}_6^{h_1h_2h_3} \approx g_s^2 S(p, 3^{h_3}, q)\mathcal{A}_4^{h_1h_2}T^{a_3}. \tag{4.2.20}$$

For the process where we have 3 gluons, we have 6 possible configurations of the helicity, which contribute to the non-vanishing amplitude $(h_1,h_2,h_3) = (-,+,+),(+,-,+),(+,+,-),(+,-,-),(-,+,-),(-,-,+)$. However, due to the factorization property, the parity of the color-ordered amplitude, and the fact that $\mathcal{A}_4^{\pm\pm} = 0$, we only have to consider the terms with $\mathcal{A}_4^{-+}$ and $\mathcal{A}_4^{+-}$,

$$\sum_{hel.}\sum_{col.} |\mathcal{A}_5|^2 \approx \frac{1}{2} g_s^2 C_F \frac{p\cdot q}{(k_3\cdot p)\,(k_3\cdot q)} \sum_{col.} \left(|\mathcal{A}_4^{-+}|^2 + |\mathcal{A}_4^{+-}|^2\right) \tag{4.2.21}$$

$$\approx \frac{1}{2} g_s^2 C_F \frac{p\cdot q}{(k_3\cdot p)\,(k_3\cdot q)} \sum_{hel.}\sum_{col.} |\mathcal{A}_4|^2. \tag{4.2.22}$$

In the last two equations, we considered the factor from the average over the helicities. Thus, for an emission of one radiated gluon, the probability density dN written in light cone coordinates, is given by

$$dN^{(1)} = \frac{1}{2} g_s^2 C_F \frac{p\cdot q}{(k_3\cdot p)\,(k_3\cdot q)} \frac{dx_3\, dk_{3_\perp}^2}{x_3}. \tag{4.2.23}$$

Using the result that we got in the previous section, involving the *soft-eikonal approximation*, we get

$$\frac{dN^{(1)}}{dx_3\, dk_{3_\perp}^2} = g_s^2 C_F \frac{1}{x_3}\frac{1}{k_{3_\perp}^2}. \tag{4.2.24}$$

This expression represents the momentum distribution for the emission of one radiative gluon. One can recognize in this expression the form of the Poisson convolution.

4.3 Two Bremsstrahlung gluons

In the general behavior of a QGP, multi-radiated gluons can be emitted. Also, in multi-gluon emission, we might expect an interference between the radiative gluons. Let us now consider the case where we have the emission of two radiated gluons (see Figure 4.3). Taking a similar approach as previously, we shall compute first the Born process $q\bar{q}gg$ with 2 Bremsstrahlung gluons and at the end apply a crossing symmetry. With the helicity choice $(--++++)$ and using the color decomposition, we have

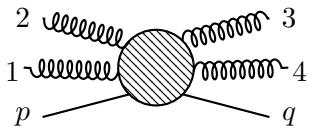

Figure 4.3: Diagrammatic representation of $q\bar{q}qg$-process with 2 Bremsstrahlung gluons.

$$\mathcal{A}_6(p^-,1^-,2^+,3^+,4^+,q^+) = g_s^4 \sum_{\sigma\in S_4} \frac{T^{a_{\sigma(1)}}T^{a_{\sigma(2)}}T^{a_{\sigma(3)}}T^{a_{\sigma(4)}}\,\langle p1\rangle^3\langle q1\rangle}{\langle p\sigma(1)\rangle\langle\sigma(1)\sigma(2)\rangle\langle\sigma(2)\sigma(3)\rangle\langle\sigma(3)\sigma(4)\rangle\langle\sigma(4)q\rangle\langle qp\rangle}. \quad (4.3.1)$$

Let us denote the color-ordered amplitude involved in the expression of the $\mathcal{A}_4$ by,

$$A_4(1,2) = \frac{\langle p2\rangle^3\langle q2\rangle}{\langle p2\rangle\langle 23\rangle\langle 3q\rangle\langle qp\rangle} \quad \text{and} \quad A_4(2,1) = \frac{\langle p2\rangle^3\langle q2\rangle}{\langle p3\rangle\langle 32\rangle\langle 2q\rangle\langle qp\rangle}. \quad (4.3.2)$$

If we expand the sum over all the permutation of the gluons in (4.3.1) we will get $4! = 24$ terms. The square of the given result will give rise to 576 terms. By taking a similar approach as previously, we can factorize the amplitude in (4.3.1) in order to get the partial amplitudes $A_{4,1}$ and $A_{4,2}$ of the parent process. Thus, $\mathcal{A}_6(p^-,1^-,2^+,3^+,4^+,q^+)$ can be rewritten as a sum of two terms, the first term contains the partial amplitudes of the parent process (with the respective color term), while the second term contains all the *extra-terms* coming from the rearrangement of the colors. To simplify the expression, let us denote $S(i,s^+,j) = S^s_{i,j}, \pi(i) = \pi_i$ and $\sigma(i) = \sigma_i$. So, we have

$$\mathcal{A}_6^{-+++} = \mathcal{A}_6(\text{parent}) + \mathcal{A}_6(\text{extra}), \quad (4.3.3)$$

where

$$\mathcal{A}_6(\text{parent}) = g_s^4 \sum_{\pi\in S_2} T^{a_{\pi_2}}T^{a_{\pi_2}}A_4(\pi_1,\pi_2)\Big[\sum_{\sigma\in S_2} T^{a_{\sigma_3}}T^{a_{\sigma_4}}\Big(S^{\sigma_3}_{\pi_2,\sigma_4}S^{\sigma_4}_{\pi_2,q} + S^{\sigma_3}_{\pi_1,\sigma_4}S^{\sigma_4}_{\pi_1,\pi_2} + S^{\sigma_3}_{\pi_1,\pi_2}S^{\sigma_4}_{\pi_2,q} + S^{\sigma_3}_{p,\pi_1}S^{\sigma_4}_{\pi_2,q} + S^{\sigma_3}_{p,\pi_1}S^{\sigma_4}_{\pi_1,\pi_2} + S^{\sigma_3}_{p,\pi_1}S^{\sigma_4}_{\sigma_3,\pi_1}\Big)\Big]. \quad (4.3.4)$$

It is worth mentioning that if we expand the sum over all the permutations we still get 24-terms. However, this expression is compact and the color terms, as well as the kinematics, are factorized in such a way that we can evaluate each term separately. On the other hand, the extra-terms are given by

$$\mathcal{A}_6(\text{extra}) = g_s^4 \sum_{\pi\in S_2} A_4(\pi_1,\pi_2)\Big[\sum_{\sigma\in S_2}\Big(T^{a_{\pi_1}}\big[T^{a_{\sigma_3}}T^{a_{\sigma_4}},T^{a_{\pi_2}}\big]S^{\sigma_3}_{\pi_1,\sigma_4}S^{\sigma_4}_{\pi_1,\pi_2} + T^{a_{\pi_1}}\big[T^{a_{\sigma_3}},T^{a_{\sigma_4}}\big] T^{a_{\pi_2}}S^{\sigma_3}_{\pi_1,\pi_2}S^{\sigma_4}_{\pi_2,q} + \big[T^{a_{\sigma_3}},T^{a_{\pi_1}}T^{a_{\pi_2}}\big]T^{a_{\sigma_4}}S^{\sigma_3}_{p,\pi_1}S^{\sigma_4}_{\pi_2,q} + T^{a_{\sigma_3}}\big[T^{a_{\pi_1}},T^{a_{\sigma_4}}\big] T^{a_{\pi_2}}S^{\sigma_3}_{p,\pi_1}S^{\sigma_4}_{\pi_1,\pi_2} + \big[T^{a_{\sigma_3}}T^{a_{\sigma_4}},T^{a_{\pi_1}}T^{a_{\pi_1}}\big]S^{\sigma_3}_{p,\pi_1}S^{\sigma_4}_{\sigma_3,\pi_1}\Big)\Big]. \quad (4.3.5)$$

The expansion of this expression will give rise to 20 terms. However, we do not even need to evaluate this expression. The reason is because, according to the kinematic parametrization, $\mathcal{A}_6(\text{extra})$ is very small and therefore can be neglected. Thus, it only remains to evaluate of the kinematic terms in (4.3.4). The contribution of the kinematic terms turns out to be very simple,

$$\mathcal{A}_6(\text{parent}) = g_s^4 \sum_{\pi\in S_2} T^{a_{\pi_1}} T^{a_{\pi_2}} A_4(\pi_1,\pi_2) \sum_{\sigma\in S_2} T^{a_{\sigma_3}} T^{a_{\sigma_4}} \frac{\langle pq\rangle}{\langle p\sigma_3\rangle\langle\sigma_3\sigma_4\rangle\langle\sigma_4 q\rangle}. \tag{4.3.6}$$

The two summations are independent, and we can recognize in the first summation the expression of the full amplitude of the Born process, thus we have

$$\mathcal{A}_6^{-+++} \approx g_s^2 \mathcal{A}_4^{-+} \sum_{\sigma\in S_2} T^{a_{\sigma_3}} T^{a_{\sigma_4}} \frac{\langle pq\rangle}{\langle p\sigma_3\rangle\langle\sigma_3\sigma_4\rangle\langle\sigma_4 q\rangle}. \tag{4.3.7}$$

Taking the square of this expression will force us to compute the following term,

$$|\mathcal{A}_6^{-+++}|^2 \approx |\mathcal{A}_4^{-+}|^2 |J(3,4)|^2, \tag{4.3.8}$$

where the square of the radiative Bremsstrahlung gluon is given by

$$|J(3,4)|^2 = g_s^4 (p\cdot q) \sum_{\sigma\in S_2} \left[\frac{T^{a_{\sigma_3}} T^{a_{\sigma_4}} T^{a_{\sigma_4}} T^{a_{\sigma_3}}}{4\,(p\cdot k_{\sigma_3})\,(k_{\sigma_3}\cdot k_{\sigma_4})\,(k_{\sigma_4}\cdot q)} - \frac{1}{k_3\cdot k_4} \frac{T^{a_{\sigma_3}} T^{a_{\sigma_4}} T^{a_{\sigma_3}} T^{a_{\sigma_4}}}{\langle\sigma_3 p\rangle[p\sigma_4]\langle\sigma_4 q\rangle[q\sigma_3]} \right]. \tag{4.3.9}$$

If we expand the sum over the permutation for the second part of this equation, the terms in the denominator are given by $\langle 3p\rangle[p4]\langle 4q\rangle[q3]$ and $\langle 4p\rangle[p3]\langle 3q\rangle[q4]$ which respectively can be written as $\langle 3p4q3]$ and $\langle 4p3q4]$. However, we saw in the previous section that $\langle 4p3q4] = \langle 3p4q3]^*$. Therefore, the expression of the amplitude squared averaged over the colors is given by

$$\begin{aligned}\sum_{col.} |\mathcal{A}_6^{-+++}|^2 \approx\; & g_s^4\, Tr(T^{a_3} T^{a_4} T^{a_4} T^{a_3} |\mathcal{A}_4^{-+}|^2) \sum_{\sigma\in S_2} \frac{p\cdot q}{4\,(p\cdot k_{\sigma_3})\,(k_{\sigma_3}\cdot k_{\sigma_4})\,(k_{\sigma_4}\cdot q)} \\ & - Tr(T^{a_3} T^{a_4} T^{a_3} T^{a_4} |\mathcal{A}_4^{-+}|^2) \frac{p\cdot q}{k_3\cdot k_4} \frac{2\mathfrak{Re}(\langle 3p4q3])}{|\langle 3p4q3]|^2}. \end{aligned} \tag{4.3.10}$$

The trace terms are given by

$$Tr(T^{a_3} T^{a_4} T^{a_4} T^{a_3} |\mathcal{A}_4^{-+}|^2) = C_F^2 Tr(|\mathcal{A}_4^{-+}|^2), \tag{4.3.11}$$

$$Tr(T^{a_3} T^{a_4} T^{a_3} T^{a_4} |\mathcal{A}_4^{-+}|^2) = -\frac{C_F}{C_A} Tr(|\mathcal{A}_4^{-+}|^2). \tag{4.3.12}$$

By virtue of these relations and equation (3.2.9), the expression in (4.3.10) can be written as

$$\sum_{col.} |\mathcal{A}_6^{-+++}|^2 \approx g_s^4 \sum_{col.} |\mathcal{A}_4^{-+}|^2 \left[C_F^2 \frac{p\cdot q}{4\,k_3\cdot k_4} \sum_{\sigma\in S_2} \frac{1}{(p\cdot k_{\sigma_3})(q\cdot k_{\sigma_4})} + \frac{C_F}{C_A} \frac{p\cdot q}{k_3\cdot k_4} \frac{Tr(\not{k}_3 \not{p} \not{k}_4 \not{q})}{|\langle 3p4q3]|^2} \right].$$

By developing the term in the denominator, $|\langle 3p4q3]|^2 = 16\,(p\cdot k_3)(p\cdot k_4)(q\cdot k_3)(q\cdot k_4)$. On the other hand, the sum over the permutation of 3 and 4 can be evaluated as:

$$\sum_{\sigma\in S_2} \frac{1}{(p\cdot k_{\sigma_3})(q\cdot k_{\sigma_4})} = \frac{(p\cdot k_3)(q\cdot k_4) + (p\cdot k_4)(q\cdot k_3)}{(p\cdot k_3)(p\cdot k_4)(q\cdot k_3)(q\cdot k_4)}. \tag{4.3.13}$$

In this expression the numerator can be rewritten as

$$(p\cdot k_3)(q\cdot k_4) + (p\cdot k_4)(q\cdot k_3) = \frac{1}{4} Tr(\not{p}\not{k}_4\not{q}\not{k}_3) + (p\cdot q)(k_3\cdot k_4). \tag{4.3.14}$$

Thus, the expression of the amplitude squared, summed over the colors, now becomes

$$\sum_{col.} |\mathcal{A}_6^{-+++}|^2 \approx g_s^4 \sum_{col.} |\mathcal{A}_4^{-+}|^2 \Bigg[\frac{C_F^2}{4} \left(\frac{p\cdot q}{(p\cdot k_3)(k_3\cdot q)} \frac{p\cdot q}{(p\cdot k_4)(k_4\cdot q)} \right) + C_F \left(C_F + \frac{1}{C_A} \right) \frac{p\cdot q}{16\, k_3\cdot k_4} \frac{Tr(\not{p}\not{k}_4\not{q}\not{k}_3)}{(p\cdot k_3)(p\cdot k_4)(q\cdot k_3)(q\cdot k_4)} \Bigg]. \tag{4.3.15}$$

The average over all possible helicities requires the computation of NMHV-amplitudes. For a process involving a single quark anti-quark pair and 4 gluons, two of the gluons have to have a negative helicity. Recall that we do not have to take into consideration the helicities of the quarks. If (h_1, h_2, h_3, h_4) denotes the helicities of the 4 gluons, there are 6 possible helicity configurations. However, we saw in the previous section that flipping helicities is equivalent to flipping labels. Thus, we are only required to compute one configuration. Using the BCFW on-shell recursion, the computation of the NHMV-amplitude can be reduced to the computation of two MHV-amplitudes. Notice that if we choose k_2 and k_3 to be the reference line ($[2,3\rangle$-shift), only two diagrams contribute to the NMHV-amplitude (see Figure 4.4).

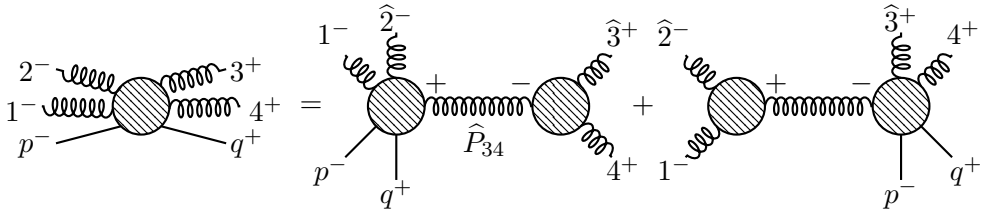

Figure 4.4: BCFW recursion for the $q\bar{q}gg$ with emission of 2 gluons in NMHV-amplitude.

The first diagram on the right-hand side is evaluated as

$$A_6^{(1)}[p^-, 1^-, 2^-, 3^+, 4^+, q^+] = A_5[p^-, 1^-, \hat{2}^-, \hat{P}_{34}^+, q^+] \frac{1}{\langle 34\rangle[34]} A_3[-\hat{P}_{34}^-, \hat{3}^+, 4^+]. \tag{4.3.16}$$

By evaluating each MHV-partial amplitude, we get

$$A_6^{(1)}[p^-, 1^-, 2^-, 3^+, 4^+, q^+] = \frac{[q\hat{P}_{34}]^3[p\hat{P}_{34}]}{[p1][1\hat{2}][\hat{2}\hat{P}_{34}][\hat{P}_{34}q][qp]} \frac{1}{\langle 34\rangle[34]} \frac{[\hat{3}4]^4}{[\hat{P}_{34}\hat{3}][\hat{3}4][4\hat{P}_{34}]}. \tag{4.3.17}$$

Notice that all the shifted momenta in this expression are only in terms of square brackets. Using the definition of the $[2,3\rangle$-shift, we can show that:

$$|\hat{P}_{34}] = \frac{\langle 23\rangle}{\langle 24\rangle}|3] + |4] \quad \text{and} \quad |\hat{2}] = |2] + \frac{\langle 34\rangle}{\langle 24\rangle}|3]. \tag{4.3.18}$$

We can now compute each term in the Equation (4.3.17). The simplest terms are $[\hat{P}_{34}\hat{3}] = [43]$ and $[4\hat{P}_{34}] = (\langle 23\rangle[43])/\langle 24\rangle$. Furthermore, we have:

$$[q\hat{P}_{34}] = -\frac{\langle 2|3+4|q]}{\langle 24\rangle},\ [p\hat{P}_{34}] = -\frac{\langle 2|3+4|p]}{\langle 24\rangle},\ [1\hat{2}] = \frac{\langle 4|2+3|1]}{\langle 24\rangle} \text{ and } [\hat{2}\hat{P}_{34}] = \frac{s_{234}}{\langle 24\rangle}, \tag{4.3.19}$$

where $s_{234} = \langle 23\rangle[23] + \langle 24\rangle[24] + \langle 34\rangle[34]$. By rearranging the expression, we get the final expression of $A_6^{(1)}$ and by taking the same approach to compute the second diagram we get the NMHV-amplitude:

$$A_6[p^-, 1^-, 2^-, 3^+, 4^+, q^+] = \frac{1}{s_{234}} \frac{\langle 2|3+4|q]^2\langle 2|3+4|p]}{\langle 23\rangle\langle 34\rangle[qp][p1]\langle 4|2+3|1]} + \frac{1}{s_{123}} \frac{[3|1+2|p\rangle^2[3|1+2|q\rangle}{[12][23]\langle pq\rangle\langle q4\rangle[1|2+3|4\rangle}. \tag{4.3.20}$$

If we expand the denominator in this expression we will get a sum of terms depending on the square and angle brackets. However, considering that $k_3 \cdot k_4, k_3 \cdot q$ and $k_4 \cdot q$ are negligibly small, all the terms in the denominator can be neglected except the largest one. In addition, the presence of 3 and 4 in the numerator makes the whole expression small compared to the MHV-partial amplitudes. One can check that all the NMHV-partial amplitudes are small compared to the leading MHV-amplitudes, and therefore can be neglected. Following the same reasoning as for the one gluon emission,

$$\sum_{hel.}\sum_{col.}|\mathcal{A}_6|^2 = \frac{g_s^4}{2}\left[\frac{C_F^2}{4}\prod_{i=3,4}\frac{p\cdot q}{(p\cdot k_i)(k_i\cdot q)}+\frac{C_A C_F}{16}\frac{(p\cdot q)Tr(\not{p}\not{k}_4\not{q}\not{k}_3)}{(k_3\cdot k_4)(p\cdot k_3)(p\cdot k_4)(q\cdot k_3)(q\cdot k_4)}\right]\sum_{hel.}\sum_{col.}|\mathcal{A}_4|^2. \tag{4.3.21}$$

To get this last expression from Equation (4.3.15) we used the fact that $C_A = N$ and did the following simplification,

$$C_F = \frac{C_A^2-1}{C_A}, \quad \text{thus} \quad C_F + \frac{1}{C_A} = C_A. \tag{4.3.22}$$

The radiation term is given by the factor in front of the parent amplitude squared, summed over the helicities and colors. One can see that two terms contribute to the expression of the radiation term. The first term, coming from the *Abelian piece*, will give the Poisson convolution. Indeed, using the parametrization defined in section 4.1, one can check that the first term gives:

$$dN(\text{Poisson}) = g_s^4\frac{C_F^2}{2}\prod_{i=3,4}\frac{dx_i}{x_i}\frac{dk_{i_\perp}^2}{k_{i_\perp}^2} = g_s^4\frac{C_F^2}{2}\frac{dx_3\,dk_{3_\perp}^2}{x_3\,k_{3_\perp}^2}\frac{dx_4\,dk_{4_\perp}^2}{x_4\,k_{4_\perp}^2}. \tag{4.3.23}$$

The second term is the *non-Abelian piece* (see Equation (4.3.24)). This term is a correction to the Poisson convolution. The distribution of the radiative gluons cannot be approximated into a Poisson distribution. Indeed, for multi-gluon emission, interference between the radiated gluons is expected.

$$dN(\text{Correction}) = g_s^4\frac{C_A C_F}{32}\frac{(p\cdot q)Tr(\not{p}\not{k}_4\not{q}\not{k}_3)}{(k_3\cdot k_4)(p\cdot k_3)(p\cdot k_4)(q\cdot k_3)(q\cdot k_4)}. \tag{4.3.24}$$

Notice that by requiring the gauge field of QCD commute, our theory will transform into QED. In that case, the correction term in the expression of the distribution of radiative gluons will tend to zero ($dN(\text{Correction}) \to 0$) and only the Poisson distribution term which has been trivially resummed in QED, will remain.

5. Conclusions

During the last decades, considerable efforts have been devoted toward the understanding of the mathematical structure of the scattering amplitudes in massless gauge theories. On the experimental side, scientists confirmed the existence of a QGP by colliding heavy nuclei (Armesto and Scomparin, 2013). This discovery opened a new area of understanding the phase diagram in QCD (Srivastava and Singh, 2012). One of the most exciting features of the heavy-ion collision is the energy loss of an energetic parton passing through the QGP. This project used the actual theory of massless gauge theories to study the radiative gluon distribution emanating from an energetic light quark.

In this work we revisited a set of tools for computing scattering amplitudes in QCD. We introduced the general color-kinematic factorization, to separate the color and the kinematic terms in the expression of scattering amplitudes (Dixon, 2014). We also introduced the spinor helicity formalism as a new variable to express scattering amplitudes. We showed that the spinor helicity formalism can be used to compute MHV-amplitudes very efficiently. This simplicity has been illustrated while computing the $ee \to \mu\mu$ process in QED. We also showed that due to the beautiful analytic structure of the scattering amplitudes, any order of amplitudes can be constructed recursively from 3-point amplitudes using the BCFW recursion. For instance, we proved that for MHV-amplitudes involving 2-quarks and a certain number of gluons, the color-ordered amplitudes have a very compact form defined by the Parke-Taylor formula (Luo and Wen, 2005).

These methods were then applied to the main focus of our work, which is the evaluation of the momentum distribution of the radiative gluons emitted from the energetic quark. For this purpose, a specific process in QCD ($qg \to qg$ process) has been considered with an emission of Bremsstrahlung gluons. It has been shown that at the amplitude level, both for the emission of 1 and 2 radiative gluons, the amplitude can be factorized into a radiative term and the amplitude of the parent process,

$$\mathcal{A}(qg \to qg + ng) \longrightarrow \mathcal{A}(qg \to qg) J(\text{radiation}), \quad n = 1, 2. \tag{5.0.1}$$

For the emission of one Bremsstrahlung gluon, when summed over the colors and the helicities, the distribution of the radiative gluon converges to the Poisson distribution,

$$\frac{dN^{(1)}}{dx_3\, dk_{3_\perp}^2} = g_s^2 C_F \frac{1}{x_3} \frac{1}{k_{3_\perp}^2}. \tag{5.0.2}$$

Notice that the parametrization set in the section 4.1 allowed us to neglect some terms in the expression of the scattering amplitude. For the case of two gluon emission, we derived the full expression of the scattering amplitude using a similar approach as in one gluon emission. The average over the final and initial colors was evaluated in the case of Maximally Helicity Violating (MHV)-amplitude. However, the average over all possible helicities needs more calculations. However, the BCFW recursion allows us to compute NMHV-amplitude via two MHV-subamplitudes. We showed that the for two gluon emission a correction term has to be added to the Poisson distribution. Therefore, we have two terms contributing to the radiative gluon distribution. The correction term is due to the interference between the two emitted radiative gluons:

$$dN^{(2)}(\text{radiation}) = dN(\text{Poisson}) + dN(\text{Correction}). \tag{5.0.3}$$

The complete evaluation of the momentum distribution for n number of radiative gluons would be a very interesting topic as a future work. Furthermore, while most of the techniques introduced in this

work are restricted in their application to tree-level, significant development has been done toward the computation of amplitudes with loops based on these techniques. The intriguing analytical properties of the scattering amplitudes led many theoretical physicists to develop further extensions of the MHV techniques such as *Twistor theory* (Witten, 2004), the *positive Grassmannian* (Arkani-Hamed et al., 2014) and the *Amplituhedron* (Arkani-Hamed and Trnka, 2014). The exploration of these techniques will help us to go beyond the Leading Order (LO) term for the computation of scattering amplitudes.

Acknowledgements

My sincere gratitude goes to Prof. Neil Turok, Prof. Barry Green and Prof. Jeff Sanders for their invaluable efforts and commitments to promote sciences in Africa through AIMS, and for the immeasurable opportunity given to me to be part of this program. I would like to express my deepest gratitude to my advisor, Dr. Horowitz for his assistance and inestimable advice. I am especially indebted to him for the time he spent assisting with this essay. I particularly acknowledge the help and suggestions provided by Nirina, thank you for being a good tutor. I would also like to thank Andriniaina Rasoanaivo for his patience and invaluable assistance. Thanks are extended to Prof. Raboanary Roland for his trust in me. Sincere thanks to the AIMS family 2016-2017, especially my *malagasy compatriots*. Finally but not least, I would like to express my sincere gratitude to my family, for their unflagging love and unconditional support throughout my life and my studies, a special thanks to Angela, Ando and Ony.

I dedicate this work to Angela Ranaivo Nambinina.

References

G. Aad et al. Observation of a centrality-dependent dijet asymmetry in lead-lead collisions at $\sqrt{s_{NN}} = 2.76\,tev$ with the ATLAS detector at the LHC. *Phys. Rev. Lett.*, 105:252303, 2010. DOI: 10.1103/PhysRevLett.105.252303.

J. Adams et al. Experimental and theoretical challenges in the search for the quark–gluon plasma: The STAR collaboration's critical assessment of the evidence from RHIC collisions. *Nucl. Phys. A*, 757(1-2):102–183, 2005. DOI: 10.1016/j.nuclphysa.2005.03.085.

S. S. Adler et al. Suppressed π_0 production at large transverse momentum in central au-au collisions at $\sqrt{s_{NN}} = 2.76\,tev$ (PHENIX collaboration). *Phys. Rev. Lett.*, 91:072301, 2003. DOI: 10.1103/PhysRevLett.91.072301.

A. Andronic et al. Heavy-flavour and quarkonium production in the LHC era: from proton–proton to heavy-ion collisions. *Eur. Phys. J. C*, 76:107, 2016. DOI: 10.1140/epjc/s10052-015-3819-5.

N. Arkani-Hamed and J. Trnka. The amplituhedron. *JHEP 1410*, 030, 2014. DOI: 10.1007/JHEP10(2014)030.

N. Arkani-Hamed, J. L. Bourjaily, F. Cachazo, A. B. Goncharov, A. Postnikov, and J. Trnka. Scattering amplitudes and the positive grassmannian. *arXiv:1212.5605 [hep-th]*, 2014.

N. Armesto and E. Scomparin. Heavy-ion collisions at the large hadron collider: A review of the results from run 1. *Eur. Phys. J. Plus*, 131:52, 2013. DOI: 10.1140/epjp/i2016-16052-4.

N. Armesto et al. Comparison of jet quenching formalisms for a quark-gluon plasma brick. *Phys.Rev. C*, 86(6):064904, 2012. DOI: 10.1103/PhysRevC.86.064904.

B. B. Back et al. The PHOBOS perspective on discoveries at RHIC. *Nucl. Phys. A*, 757(1-2):28–101, 2005. DOI: 10.1016/j.nuclphysa.2005.03.084.

R. Baier, D. Schiff, and B. G. Zakharov. Components of the dilepton continuum in pb-pb collisions at $\sqrt{s_{NN}} = 2.76\,tev$. *Annu. Rev. Nucl. Part. Sci.*, 50:37–69, 2000. DOI: 10.1146/annurev.nucl.50.1.37.

J. D. Bjorken. Energy loss of energetic partons in quarkgluon plasma: Possible extinction of high pt jets in hadron-hadron collisions. *FERMILAB-PUB-82-059-THY*, 1982.

R. Britto. Introduction to scattering amplitudes lecture 1: QCD and the spinor-helicity formalism. 2015.

S. Cao, G. Y. Qin, S. A. Bass, and B. Müller. Collisional vs. radiative energy loss of heavy quark in a hot and dense nuclear matter. *Nucl. Phys. A*, 904-905:653c–656c, 2013. DOI: 10.1016/j.nuclphysa.2013.02.100.

X. F. Chen, E. W. C. Greiner, X. N. Wang, and Z. Xu. Bulk matter evolution and extraction of jet transport parameters in heavy-ion collisions at energies available at the BNL relativistic heavy ion collider (RHIC). *Phys. Rev. C*, 81(6):064908, 2010. DOI: 10.1103/PhysRevC.81.064908.

J. C. Collins and M. J. Perry. Superdense matter: neutrons or asymptotically free quarks? *Phys. Rev. Lett.*, 34:1353, 1975. DOI: 10.1103/PhysRevLett.34.1353.

L. J. Dixon. A brief introduction to modern amplitude methods. *arXiv:1310.5353 [hep-ph] SLAC-PUB-15775*, 2014. DOI: 10.5170/CERN-2014-008.31.

B. Feng and M. Luo. An introduction to on-shell recursion relations. *Front. Phys.*, 7:533:533–575, 2012. DOI: 10.1007/s11467-012-0270-z.

O. Fochler, Z. Xu, and C. Greiner. Towards a unified understanding of jet quenching and elliptic flow within a perturbative QCD parton transport. *Phys. Rev. Lett.*, 102:202301, 2009. DOI: 10.1103/PhysRevLett.102.202301.

D. J. Gross and F. Wilczek. Ultraviolet behavior of non-abelian gauge theories. *Phys. Rev. Lett.*, 30: 1343, 1973. DOI: 10.1103/PhysRevLett.30.1343.

U. . Heinz and M. Jacob. Evidence for a new state of matter: An assessment of the results from the CERN lead beam programme. *nucl-th*, 0704:0002042, 2000.

J. M. Henn and J. C. Plefka. *Scattering amplitudes in gauge theories*. Springer, 2014. DOI: 10.1007/978-3-642-54022-6.

B. Jacak and P. Steinberg. Creating the perfect liquid in heavy-ion collisions. *Physics today*, 63N5:39, 2010. DOI: 10.1063/1.3431330.

P. Kovtun, D. T. Son, and A. O. Starinets. Viscosity in strongly interacting quantum field theories from black hole physics. *Phys. Rev. Lett.*, 94:111601, 2005. DOI: 10.1103/PhysRevLett.94.111601.

M. Luo and C. Wen. Recursion relations for tree amplitudes in super gauge theories. *JHEP*, 0503:004, 2005. arXiv:hep-th/0501121v6.

F. Maltoni, K. paul, T. Stelzer, and S. Willenbrock. An analytical study of jet cross-section in proton-proton interactions. *Phys.Rev. D*, 67, 2014. DOI: 10.1103/PhysRevD.67.014026.

S. J. Parke and M. L. Mangano. Multi-parton amplitudes in gauge theories. *Phys. Rept.*, 200:301–367, 1991. DOI: 10.1016/0370-1573(91)90091-Y.

H. D. Politzer. Reliable perturbative results for strong interactions? *Phys. Rev. Lett.*, 30:1346, 1973. DOI: 10.1103/PhysRevLett.30.1346.

C. Schwinn and S. Weinzierl. On-shell recursion relations for all born QCD amplitudes. *JHEP 0704*, 072 hep-ph/0703021 [HEP-PH] MZ-TH-07-02, PITHA-07-01, 2007.

P. K. Srivastava and C. P. Singh. Hybrid model for QCD deconfining phase boundary. *Phys. Rev. D*, 114016, 2012. DOI: 10.1103/PhysRevD.85.114016.

H. P. Trivedi, P. Bhatt, A. Kumar, L. K. Gupta, J. P. Gupta, K. Chandra, T. S. Saini, and A. Kansal. An analytical study of jet cross-section in proton-proton interactions. *DAE-BRNS symposium on nuclear physics*, V. 59:758–759, 2014.

I. Vitev. Testing the theory of QGP-induced energy loss at RHIC and the LHC. *Phys. Lett. B*, 639(3): 38–45, 2006. DOI: 10.1016/j.physletb.2006.05.083.

X.-N. Wang. Why the observed jet quenching at RHIC is due to parton energy loss. *Phys. Let. B*, 579(3,4):299–308, 2004. DOI: 10.1016/j.physletb.2003.11.011.

X. N. Wang. High $p_\perp$ hadron spectra, azimutal anisotropy and back-to-back correlations in high-energy heavy-ion collisions. *Phys. Lett. B*, 595:165, 2005. DOI: 10.1016/j.physletb.2004.05.021.

S. Wicks, W. A. Horowitz, M. Djordjevic, and M. Gyulassy. Heavy quark jet tomography of pb+pb at LHC: AdS/CFT drag or pQCD energy loss? *Nucl. Phys. A*, 784:426–442, 2007. DOI: 10.1016/j.nuclphysa.2006.12.048.

E. Witten. Perturbative theory as a string theory in twistor space. *Commun. Math. Phys.*, 252:189–258, 2004. DOI: 10.1007/s00220-004-1187-3.

A. Zee. *Quantum Field theory in a Nutshell, 2nd edition*. Princeton University Press, ISBN-13: 978-0691140346, 2010. ISBN: 978-0-691-14034-6.